

## Intense reducing conditions during the last deglaciation and Heinrich events (H1, H2, H3) in sediments from the oxygen minimum zone off Goa, eastern Arabian Sea

J.N. Pattan\*, G. Parthiban., Anita Garg., N.R. Cesar Moraes.

CSIR-National Institute of Oceanography,  
Dona Paula, 403 004, Goa, India.

\*e-mail: [pattan@nio.org](mailto:pattan@nio.org)  
Phone: 91-832-2450360

### ABSTRACT

#### Abstract

Two sediment cores, ABP-32/GC-01R and ABP-32/GC-03 were collected at a water depth of 642m and 1086m off Goa from the present day Oxygen Minimum Zone (OMZ) of eastern Arabian Sea (EAS) cover time span of last 18 ka and 32 ka respectively were analysed for multi-proxy redox-sensitive elements to understand the variation in the redox conditions and factors responsible for its development.

Redox-sensitive elements concentration and their normalized ratios (Mn/Al, U/Th, Mo/Al and Ce/Ce\*) suggest that sediment core ABP-32/GC-01R is under more reducing conditions due to its location within the centre of OMZ compared to core ABP-32/GC-03 which is at the base of OMZ. Sediments from the EAS are of non-euxinic environments where dissolved sulfide is present but restricted to the sediment pore-waters. Lack of significant correlation ( $r < 0.1$ ) of organic carbon with U and Mo suggest that productivity may not have control on the development of reducing conditions. The lowest Mn/Al ratio, strong negative Ce/Ce\* anomaly and remarkable enrichment of U/Th and Mo/Al ratios during the last deglaciation, and Heinrich events (H1, H2, H3) indicate intense reducing conditions probably due to poor ventilation by oxygen depleted bottom waters from Subantarctic Mode Waters (SAMW) - Antarctic Intermediate waters (AAIW). There is a distinct lanthanide fractionation in the sediment cores where,  $L_{a(n)}/Yb_{(n)}$  ratio is  $< 1$ ,  $\approx 1$  and  $> 1$  during the last 10 ka (Holocene), 14 - 10 ka (includes-Younger Dryas and Bölling-Alleröd), 18-14 ka (last deglaciation) and Heinrich events suggesting less reducing, terrigenous dominated and intense reducing condition respectively.

**Keywords:** Eastern Arabian Sea sediments, Oxygen Minimum Zone, redox-sensitive elements, non-euxinic, reducing conditions, last deglaciation, Heinrich events (H1, H2, H3), ventilation, lanthanide fractionation.

#### – Research highlights:

Formatted: Font: Italic

Formatted: Indent: Left: 0"

Formatted: Font: (Default) Times New Roman, 12 pt, Italic, Complex Script Font: Times New Roman, 12 pt

Formatted: Left: 0.75", Right: 0.75", Width: 8.27", Height: 11.69"

Formatted: Font: 13 pt, Complex Script Font: 13 pt

Formatted: Centered, Indent: Left: 0", Line spacing: single

Formatted: Font: Bold

Formatted: Font: 13 pt, Complex Script Font: 13 pt

Formatted: Font: 13 pt, Complex Script Font: 13 pt

Formatted: Font: 13 pt, Bold, Complex Script Font: 13 pt

Formatted: Font: Bold

Formatted: Indent: Left: 0", Line spacing: single

Formatted: Font: 12 pt, Bold, Complex Script Font: 12 pt

Formatted: Font: 12 pt, Complex Script Font: 12 pt

Formatted: Font: 12 pt, No underline, Font color: Auto, Complex Script Font: 12 pt

Formatted: Font: 12 pt, Complex Script Font: 12 pt

Formatted: Font: 12 pt, No underline, Font color: Auto, Complex Script Font: 12 pt

Formatted: Font: 12 pt, Complex Script Font: 12 pt

Formatted: Font: 12 pt, Bold, Complex Script Font: 12 pt

Formatted: Justified, Space After: 6 pt

Formatted: Font: 12 pt, Bold, No underline, Font color: Auto, Complex Script Font: 12 pt

Formatted: Justified, Indent: Left: 0", Space After: 6 pt

Formatted: Font: 12 pt, Bold, Complex Script Font: 12 pt

Formatted: Font: 12 pt, No underline, Font color: Auto, Complex Script Font: 12 pt

Formatted: Font: 12 pt, Complex Script Font: 12 pt

Formatted: Font: Bold

Formatted: Font: 12 pt, Bold, Complex Script Font: 12 pt

Formatted: Space After: 6 pt, Line spacing: single

Formatted: Indent: Left: 0", First line: 0.5", Space After: 6 pt, Line spacing: single

Formatted: Space After: 6 pt, Line spacing: single

Formatted: Indent: First line: 0.44", Space After: 6 pt, Line spacing: single

Formatted: Font: Not Italic

Formatted: Justified, Space After: 6 pt, Line spacing: single

Formatted: Justified, Space After: 6 pt

Formatted: Justified, Indent: Left: 0", Space After: 6 pt

Formatted: Justified, Space After: 6 pt

Formatted: Font: 12 pt, Not Italic, Complex Script Font: 12 pt

Sediments from eastern Arabian Sea are of non-euxinic environments where hydrogen sulfide is restricted to sediment pore-waters.

Productivity may not have control on the development of reducing conditions.

Intense reducing conditions during last deglaciation and Heinrich events(H1, H2, H3) could be due to ventilation of the oxygen depleted bottom waters from SAIW-AAIW:

There is distinct lanthanide fractionation [ $La_{(n)}/Yb_{(n)}$ ] in the last 10 ka (Holocene), 14- 10 ka (Younger dryas, Bølling-Allerød) and 18-14 ka (last deglaciation) are associated with less reducing, terrigenous dominated and intense reducing conditions respectively.

## Introduction

The concentration of trace metals in marine sediments reflect the geochemical process controlling their supply, distribution, and process of removal from the ocean (Rosenthal et al., 1995). The distribution pattern of redox-sensitive elements is mainly related to degradation of organic matter during its settling and diagenesis and also oxygen concentrations in the bottom waters (i.e., ventilation) at the time of sediment deposition on the seafloor. The degradation sequence of organic matter starts with consuming free molecular oxygen, followed in sequence by the reduction of nitrate, manganese, reactive iron, sulfate, and carbon dioxide (Froelich et al., 1979; Canfield and Thamdrup, 2009). At each reduction stage the behavior and distribution of redox-sensitive elements is variable. The behavior of redox-sensitive elements change at relatively low oxygen content and their behavior varies with local sedimentary environment. Organic carbon rich marine sediments

Formatted: Font: 12 pt, Complex Script Font: 12 pt

Formatted: Justified, Indent: First line: 0", Space After: 6 pt

Formatted: Font: Not Italic

Formatted: Space After: 6 pt

Formatted: Font: Not Italic, No underline, Font color: Auto

Formatted: Font: Not Italic

Formatted: Font: Not Italic, No underline, Font color: Auto

Formatted: Font: Not Italic

Formatted: Font: Not Italic, No underline, Font color: Auto

Formatted: Font: Not Italic

Formatted: Font: 12 pt, Complex Script Font: 12 pt

Formatted: Font: Not Italic

Formatted: Indent: Left: -0.38", Space After: 6 pt, No bullets or numbering

Formatted: Font: Not Italic, No underline, Font color: Auto

Formatted: Font: Not Italic

Formatted: Font: 12 pt, Not Bold, Complex Script Font: 12 pt

Formatted: Justified, Indent: Left: 0", Space After: 6 pt, Line spacing: 1.5 lines

Formatted: Font: Not Italic

Formatted: Font: 12 pt, No underline, Font color: Auto, Complex Script Font: 12 pt

Formatted: Justified, Indent: Left: 0", Space After: 6 pt, Line spacing: 1.5 lines

Formatted: Font: 12 pt, Complex Script Font: 12 pt

Formatted: Space After: 6 pt, Line spacing: 1.5 lines

Formatted: Font: 12 pt, No underline, Font color: Auto, Complex Script Font: 12 pt

Formatted: Space After: 6 pt

are generally characterized by the enrichment of a number of minor and trace elements and they can be used as paleo-redox and paleo-productivity proxies (e.g., Tribovillard et al., 2006; Calvert and Pedersen 2007; McKay and Pedersen, 2014). Redox-sensitive elements such as bulk U and Mo concentrations and ratios such as U/Th and Mo/Al tend to be enriched under reducing conditions making useful proxies to understand the paleo-redox conditions (Algeo and Tribovillard, 2012; Algeo and Rowe, 2012). Under suboxic conditions, Re and U are enriched (~10 ppb and ~5 ppm respectively) by their reduction and subsequent precipitation (Crusius et al., 1996; Morford et al., 2012), while under anoxic conditions Mo enrichment is moderate (up to ~20 ppm) when pore water is sulfidic, becoming highly enriched (>60 ppm) under euxinic conditions (Scott and Lyons, 2012). The redox-conditions under which these metals accumulate and the mechanisms responsible for their accumulation differ greatly (McKay and Pedersen, 2014). Under oxic conditions, both manganese ( $Mn^{4+}$ ) and Molybdenum ( $Mo^{6+}$ ) are enriched, and Mo is associated with Mn-oxhydroxides where Mo/Mn ratio remains constant of 0.002 (Shimmiel and Price, 1986). Cerium (Ce) is a unique member of lanthanide group due to its dual oxidation state and Ce-anomaly is negative under reducing conditions while, it is positive under oxic conditions (German and Elderfield, 1990) and making its usefulness to reconstruct the paleo-redox conditions. Therefore sedimentary redox chemistry is a common method to reconstruct the past bottom water oxygen conditions. In addition to redox-sensitive element concentrations, other parameters such as benthic faunal assemblages, the presence or absence of laminated sediments, and  $\delta^{15}N$  of bulk sediments are sensitive to oxygen concentration at the sediment-water interface (Jaccard and Galbraith, 2011).

In the Arabian Sea, productivity estimated from the sediment trap data (~200g  $cm^{-2}$  of C.) is generally high (Nair et al., 1989) and of which nearly 70-80% of biogenic material is deposited during summer monsoon. It was suggested that summer monsoon was stronger during interglacial than in the cold glacial periods (Prell and Kutzbach, 1987; Pattan et al., 2003; Banakar et al., 2005 and reference therein). Different parts of Arabian Sea has experienced large regional variation in productivity pattern during different seasons. In the western Arabian Sea, winds associated with summer monsoon drive productivity (Levy et al., 2007) whereas in the northern and central Arabian Sea it is due to intense convective mixing and deepening of mixed layer during the winter monsoon (Madhupratap et al., 1996). In the Arabian Sea, the combined effect of high surface water productivity, intense carbon respiration in the water column and intermediate water circulation responsible for the development of Oxygen Minimum Zone between 150 and 1250 m water depth

Formatted: Font: 12 pt, Complex Script Font: 12 pt

Formatted: Font: 12 pt, No underline, Font color: Auto, Complex Script Font: 12 pt

(Wyrтки, 1973). Productivity is responsible for the development of reducing conditions along with ventilation and rapid sedimentation rate (McKay and Pedersen, 2014).

Formatted: Font: 12 pt, Complex Script Font: 12 pt

The climatic events during the last 30 ka includes Heinrich events (H1: 17-15ka, H2: 25-23ka and H3: 30-29ka) where large armdas of icebergs break off from glaciers and travers in North Atlantic, Last Glacial Maximum (LGM ~23 to 19 ka) where Ice Sheets were at their greatest extension, followed by last deglaciation (LDG ~18 to 14ka), then a warm and moist inter stadial period of Bólling-Alleród (~14.7 to 12.7 ka), Younger Dryas (YD) cold event (~12.9 to 11.6 ka) and the Holocene covers the last ~10 ka. It is important to know the redox conditions during these climatic events in the eastern Arabian Sea.

Formatted: Font: 12 pt, No underline, Font color: Auto, Complex Script Font: 12 pt

Studies related to the sediment depositional history in the EAS, particularly those based on redox-sensitive elements, are very sparse (Sarkar et al., 1993; Pattan and Pearce, 2009). These investigations are confined to southeastern Arabian Sea particularly from deep waters of ~2300m depth and they proposed suboxic to near anoxic conditions occurred during last glacial cycle and LGM caused by change in deep water circulation.. However, there are no studies related to redox conditions using multiple redox-sensitive elements from the eastern Arabian Sea from shallow water depth particularly within the present day Oxygen Minimum Zone. Therefore in the present study, we have used a multi-proxy approach with number of redox-sensitive elements (Mn, Fe, U, Mo and Ce), which behave differently under oxidic, suboxic, and anoxic conditions. The objective of the present study is to understand the variation in redox conditions and factors responsible for its development by utilizing two sediment cores located at a water depths of 642m and 1086m within the present day Oxygen Minimum Zone during the last 32 ka from EAS.

Formatted: Font: 12 pt, Complex Script Font: 12 pt

Formatted: Font: 12 pt, No underline, Font color: Auto, Complex Script Font: 12 pt

Formatted: Font: 12 pt, Complex Script Font: 12 pt

Formatted: Space After: 6 pt

## 2. Materials and Methods

During the *Akademik Boris Petrov* cruise number 32 in 2008, two sediment cores ABP-32/GC-01R and ABP-32/GC-03 were retrieved off Goa, EAS at a water depth of 642m and 1086m respectively. Both the sediment cores are situated in the present day Oxygen Minimum Zone (150-1200m). Sediment core ABP-32/GC-01R is referred to as GC-01R and ABP-32/GC-03 as GC-03 in the subsequent text. Sediment core locations are shown in Figure 1 and their details are presented in Table 1.

Formatted: Font: 12 pt, No underline, Font color: Auto, Complex Script Font: 12 pt

Formatted: Font: 12 pt, Complex Script Font: 12 pt

Formatted: Font: 12 pt, No underline, Font color: Auto, Complex Script Font: 12 pt

Formatted: Font: 12 pt, Complex Script Font: 12 pt

Both the sediment cores were sub-sampled onboard at 2 cm intervals. Sediment subsamples were dried and finely powdered. A total of 102 and 80 subsamples from GC-01R and GC-03 are used in the present study respectively. About 10 g of bulk sediment was soaked in water overnight then, it was sieved with 63 micron sieve for coarse fraction. AMS radiocarbon dates were obtained from National Science Foundation -Arizona AMS Facility, utilizing single planktonic species (*G. Sacculifer*, 250-350 $\mu$ m size-fraction) from the + 63 micron coarse fraction. Radiocarbon dates were converted to calendar age (ka) using the CalPal2007-HuLu calibration of QuickCal 2007 version 1.5 (Danzeglocke et al., 2011) and were corrected for reservoir effects (622yr) based on the Indian Ocean reservoir corrections suggested by Southon et al. (2002).

Formatted: Font: 12 pt, No underline, Font color: Auto, Complex Script Font: 12 pt

Bulk sediments were treated with 1N HCl to remove the calcium carbonate fraction. Carbonate-free aliquots were analyzed for Organic Carbon ( $C_{org}$ ), Organic Nitrogen ( $N_{org}$ ). Concentrations of  $C_{org}$  and  $N_{org}$  were determined by combusting pre-weighed carbonate free aliquots in an elemental analyzer (Thermo Electron Corporation, Flash EA, 1112). Calibration for  $C_{org}$  and  $N_{org}$  analysis was carried out using 2, 5-bis-(5-tetrabutyl-benzoxazol-2-yl) thiopen (BBOT) as a standard. The analytical precision for replicate samples was within  $\pm 1.6\%$  for  $C_{org}$  and  $\pm 1.8\%$  for  $N_{org}$ .

Formatted: Font: 12 pt, Complex Script Font: 12 pt

Formatted: Font: 12 pt, No underline, Font color: Auto, Complex Script Font: 12 pt

Calcium carbonate content was determined with a coulometer (UIC, Inc-CM5130 acidification module). Analytical grade calcium carbonate was used as a standard reference material. The accuracy and precision of measurements were better than  $\pm 2\%$ . Dried and powdered sediment (0.5 g) was mixed with Merck's Spectromelt<sup>®</sup> A12 Flux and borate beads were prepared in a Minifuse 2 induction furnace at  $\sim 1000\text{ }^{\circ}\text{C}$ . These beads were used to determine the major elements by X-ray fluorescence (PANalytical Axios). Accuracy and precision of the data was checked with international standard reference materials (MAG-1 and JMS-1), and was better than  $\pm 4\%$ .

Formatted: Font: 12 pt, Complex Script Font: 12 pt

Formatted: Font: 12 pt, No underline, Font color: Auto, Complex Script Font: 12 pt

For trace element analysis, about 50 mg of sediment was weighed into a teflon beaker. To this a 10 ml of acid mixture of HF+HNO<sub>3</sub>+HClO<sub>4</sub> (7:3:1) was added and heated on a hot plate at a temperature of 180  $^{\circ}\text{C}$  until it became paste. Another aliquot of same acid mixture (10 ml) was added, and heated again till it became paste. To this paste, 4 ml of 1:1 HNO<sub>3</sub> was added and heated for 5 minutes then diluted to 100 ml with ultrapure water (18.2 M $\Omega$ ). A standard reference material (MAG-1), blanks and duplicates were also prepared in the same way as sediment samples. All the acids used were of supra pure quality. The digested solutions were measured for trace elements on an inductively coupled plasma-mass spectrometer (Thermo X-Series 2) at National Institute of Oceanography, Goa, India. The accuracy and precision of the data were better than  $\pm 6\%$ . Element

Formatted: Font: 12 pt, Complex Script Font: 12 pt

Formatted: Font: 12 pt, No underline, Font color: Auto, Complex Script Font: 12 pt

concentration is reported on carbonate free basis (CFB) using equation (Element con X (1- CaCO<sub>3</sub> %/100) .

The Ce/Ce\* anomaly has been calculated as  $Ce/Ce^* = 2 \times Ce_{(n)} / (La_{(n)} + Pr_{(n)})$  where n is shale-normalized value.

### 3. Results and discussion

#### 3.1. Age model and sedimentation rates

Radiocarbon measurements suggest that GC-01R covers a time span of ~0-18 ka and GC-03 covers ~0-32 ka respectively (Table 2). GC-01R had a sediment accumulation rate of 12.6 cm/ka during Holocene and increased by nearly three times (35 cm/ka) during Marine Isotope Stage (MIS)-2 (Fig 2a). GC-03 also had a low sedimentation rate during Holocene (9.7 cm/ka) and increased to 14.2 cm/ka during MIS-2 (Fig. 2b). Therefore, the sedimentation rates obtained for the Holocene periods in both the cores is lower than those recorded during MIS-2.

#### 3.2 Past productivity changes

The accumulation of calcium carbonate in the marine sediments is mainly controlled by the productivity in the euphotic zone, the rate of dissolution during transit to seafloor and burial, and dilution by the non-carbonate material such as detrital silicates (Volat et al., 1980). Calcium carbonate content is high in core GC- 01R (27-79 %) compared to GC-03 (27-67%: Fig. 3). However, its distribution pattern in both the sediment core is similar. Calcium carbonate content varies from 35-40 % over the last 10 ka (Holocene), reached lowest of ~30% between 10 and 14 ka and reached maximum of 67-79 % during 18 to 14 ka (last deglaciation), and also during Heinrich events H2 and H3 (Fig.3). Increased calcium carbonate content during last deglaciation

Formatted: Font: 12 pt, Complex Script Font: 12 pt

Formatted: Font: 12 pt, No underline, Font color: Auto, Complex Script Font: 12 pt

Formatted: Font: 12 pt, Complex Script Font: 12 pt

Formatted: Font: 12 pt, No underline, Font color: Auto, Complex Script Font: 12 pt

Formatted: Font: 12 pt, Complex Script Font: 12 pt

Formatted: Justified, Space After: 6 pt, Line spacing: 1.5 lines

Formatted: Justified, Indent: Left: 0", Space After: 6 pt, Line spacing: 1.5 lines

Formatted: Font: 12 pt, No underline, Font color: Auto, Complex Script Font: 12 pt

Formatted: Justified, Space After: 6 pt, Line spacing: 1.5 lines

Formatted: Font: 12 pt, Complex Script Font: 12 pt

Formatted: Font: 12 pt, No underline, Font color: Auto, Complex Script Font: 12 pt

Formatted: Justified, Space After: 6 pt, Line spacing: 1.5 lines

Formatted: Font: 12 pt, Complex Script Font: 12 pt

Formatted: Font: 12 pt, No underline, Font color: Auto, Complex Script Font: 12 pt

Formatted: Space After: 6 pt

Formatted: Font: 12 pt, Complex Script Font: 12 pt

Formatted: Font: 12 pt, No underline, Font color: Auto, Complex Script Font: 12 pt

Formatted: Space After: 6 pt

Formatted: Font: 12 pt, Complex Script Font: 12 pt

Formatted: Font: 12 pt, No underline, Font color: Auto, Complex Script Font: 12 pt

and Heinrich events is corroborated with high aragonite and pteropods abundance suggesting better preservation in the EAS rather than the high productivity (Naidu et al., 2013). This in-turn reflect increased deep-water carbonate ion concentration and associated deep water circulation (Naik and Naidu, 2016). Therefore, high carbonate content during last deglaciation and Heinrich events in the present sediment cores do not represent high productivity. Based on number of studies, it is observed that calcium carbonate behavior is different during last deglaciation and Heinrich events within the Arabian Sea. For example, in the EAS particularly sediments from north off Goa coast, calcium carbonate is high during last deglaciation and Heinrich events (Ivanochko, 2004; Bonning and Bard, 2009) whereas, Mir Ahmad et al (2013) recorded increased carbonate during last deglaciation and H3 but not in the H2. On the contrary, carbonate peaks are missing during last deglaciation and Heinrich events in the several sediment cores from southeastern Arabian Sea particularly south off Goa (Pattan et al., 2003; Agnihotri et al., 2003; Narayana et al., 2009; Saraswat et al., 2013; Naik et al., in press). Therefore, Arabian Sea is not exception to the missing carbonate peaks during last deglaciation and Heinrich events like other several sediment cores from the world Oceans (Mekik et al., 2012).

Formatted: Font: 12 pt, Complex Script Font: 12 pt

Aluminium (Al) in the marine sediment represents mostly terrigenous source and its abundance is associated with the intensity of monsoons. Al content varies from 4 to 11 % and 8 to 11 % in GC-01R and GC-03 respectively (Fig.3). During Holocene Al content is almost uniform (~ 9 %) and increased to maximum during ~14 to 10 ka (10-11 %) and from there reached to minimum during last deglaciation and Heinrich events. Highest carbonate content during last deglaciation and Heinrich events is associated with lowest Al suggesting dilution effect.

Formatted: Font: 12 pt, No underline, Font color: Auto, Complex Script Font: 12 pt

The content and type of organic matter present in the marine sediments will reflect the supply and method of its preservation. However, what controls the accumulation and preservation of organic matter in Arabian Sea sediments (i.e., surface productivity and/or to oxygen content of the water column) is still an enigma. Organic carbon ( $C_{org}$ ) content in GC-01R varies considerably from 0.8 to 10 % with its high concentration of 8 to 10% during late Holocene (last 4 ka) and gradually decreased from 8 to 3 % from 6 to 4 ka (Fig. 3). Therefore, increased  $C_{org}$  during the last 6 ka may represent high productivity. Lowest  $C_{org}$  is recorded from 14-6 ka, during last deglaciation and Heinrich events in both the sediment cores.  $C_{org}$  content is low (1 to 4.2 %) in GC-03 compared to GC-01R (0.8 to 10 %). In both the sediment cores the C/N ratio is ~10 and  $\delta^{13}C$  is -18.9 to -23.4 ‰ suggesting that organic carbon is of marine origin during the last 32 ka in EAS (Pattan, unpublished data).

Formatted: Font: 12 pt, Complex Script Font: 12 pt

Formatted: Font: 12 pt, No underline, Font color: Auto, Complex Script Font: 12 pt

Formatted: Font: 12 pt, Complex Script Font: 12 pt

The large variation of  $C_{org}$  in GC-01R (0.8 to 10 %) and GC-03 (1 to 4.2 %) suggest its degradation with time. To understand this, we have calculated the  $C_{org}:P_{tot}$  molar ratio, and it varies from 10 to 50, and is lower than the Redfield ratio of 106 (Fig. 5). This ratio reached minimum during last deglaciation and Heinrich events probably due to degradation of labile organic carbon occurred more effectively or there was differential water column respiration as particles were settling (Paytan and McLaughlin, 2007). Algeo and Ingall (2007) summarized the  $C_{org}:P$  molar ratio in the modern marine sediments and their relationship to bottom water redox conditions. They suggested this ratio will be highest (~150 to ~200) for permanently anoxic basin, ~75 to ~130 for suboxic to intermittently anoxic environments and < 40 for the oxic to suboxic conditions. In both the sediment cores the mean  $C_{org}:P$  molar ratio is 27 and fall within oxic to suboxic environment (Algeo and Ingall, 2007) and are nearly similar to Nambian shelf (~40), Amazon shelf (<30) and Blake Plateau (<30) (Yuan 2017-In press).

Formatted: Font: 12 pt, No underline, Font color: Auto, Complex Script Font: 12 pt  
Formatted: Space After: 6 pt

Ba/Al ratio or  $Ba_{exc}$  in the marine sediments has been proved to be a better indicator of productivity because of its post-depositional refractory nature (Dymond et al., 1992; Gingle et al., 1999). Ba/Al ratio varies from 0.003 to 0.012 in the sediment cores (Fig.3). High Ba/Al ratio (up to 0.012) above the upper continental crust (0.0068) during late Holocene indicates higher productivity. Ba/Al ratio remains low and almost constant (~0.004) and below the upper continental crust from 32 to 8 ka. There is a positive correlation between  $C_{org}$  and Ba in both the cores (Table 3 & 4) suggesting productivity. However, correlation between calcium carbonate and  $C_{org}$  is not consistent in both the cores (Table 3 & 4).  $C_{org}$  and Ba/Al ratio in the EAS indicates high productivity during the late Holocene (last 6 ka) and high carbonate during last deglaciation and Heinrich events suggest better carbonate preservation rather than productivity.

Formatted: Font: 12 pt, Complex Script Font: 12 pt  
Formatted: Font: 12 pt, No underline, Font color: Auto, Complex Script Font: 12 pt

### 3.3 Past changes in bottom water oxygenation

Formatted: Font: 12 pt, Complex Script Font: 12 pt  
Formatted: Justified, Space After: 6 pt, Line spacing: 1.5 lines

#### 3.3.1 Manganese and iron

Formatted: Font: 12 pt, No underline, Font color: Auto, Complex Script Font: 12 pt  
Formatted: Justified, Space After: 6 pt, Line spacing: 1.5 lines  
Formatted: Font: 12 pt, Complex Script Font: 12 pt  
Formatted: Font: 12 pt, No underline, Font color: Auto, Complex Script Font: 12 pt  
Formatted: Justified, Space After: 6 pt, Line spacing: 1.5 lines  
Formatted: Font: 12 pt, Complex Script Font: 12 pt



Manganese is a redox-sensitive element and present as  $Mn^{4+}$  in oxic environments, whereas under reducing conditions  $Mn^{4+}$  dissolves into pore water as  $Mn^{2+}$ , diffuses upwards and subsequently re-precipitated as  $Mn^{4+}$  (Lynn and Bonatti, 1965). However, if surface sediments are suboxic  $Mn^{2+}$  may be lost to the overlying water column (Calvert and Pedersen, 1994). Bulk Mn concentration in both sediment cores show large fluctuations ranging from 30 to 560 ppm and is lower than the upper continental crustal value of 600 ppm (McLennan, 2001). The highest Mn content (330-560 ppm) occurred from 14 to 10 ka and the lowest (30 ppm) during last deglaciation and Heinrich events. The Mn/Al ratio in GC-01R varies from 0.0004 to 0.005, and in GC-03, ranges from 0.001 to 0.005 (Fig. 4). These ratios are low compared to those of upper continent crust (0.0085; McLennan, 2001), suggesting reducing conditions. The relatively high Mn/Al ratio (0.005 to 0.055) from 14 to 9 ka may represent comparatively less reducing conditions with rest of the sediment core and in-turn may suggest inflow of oxygenated waters. The time period of 14-9 ka includes the cooler Younger Dryas (12.9 to 11.6 ka) and warm Bølling-Allerød (14.7 to 12.7 ka). Based on the high aragonite content and more shell weight of planktonic foraminifera *G. ruber* during YD in the eastern Arabian Sea suggested presence of oxygenated Subantarctic Mode Water (SAMW) and Antarctic Intermediate Waters (AAIW) (Singh, 2007; Naik et al. 2014).

Formatted: Font: 12 pt, No underline, Font color: Auto, Complex Script Font: 12 pt

Formatted: Space After: 6 pt

Iron content varies from 3.4 to 8.7 % (avg. 6.9 %) and 5.0 to 7.9% (avg. 6.3%) in GC-01R and GC-03 respectively. Fe/Al ratio ranges from 0.58 to 0.83 in GC-01R and 0.57 to 0.79 in GC-03 (Fig. 4) and is always higher than the average upper continental crust value of 0.43 (McLennan, 2001). This could be due to fact that there is an additional supply of Fe other than that of aluminosilicates. The Fe content and Fe/Al ratio from 14 to 10 ka is highest and nearly double compared that of upper continental crust, reflecting a greater supply of Fe-rich material. Even though, Fe/Al ratio reached minimum during last deglaciation, still it is higher than the upper continental crust ratio. The distribution pattern of Fe/Al is nearly similar to that of Mn/Al in both the sediment cores (Fig. 4). The Fe/Al ratio in the sediments from the OMZ of EAS is quite different from that of the Peru continental margin, which has one of the most pronounced OMZs in the world oceans. Sedimentary Fe is depleted compared to upper continental crust within the OMZ and enriched outside of the OMZ because Fe is reductively remobilized from sediments within the OMZ and then laterally transported and re-precipitated in more oxic water outside the OMZ (Scholz et al., 2014). Such Fe reduction is not observed in the EAS, even though Mn dissolution has

Formatted: Font: 12 pt, Complex Script Font: 12 pt

Formatted: Font: 12 pt, No underline, Font color: Auto, Complex Script Font: 12 pt

occurred in both the cores. The high Fe content in these sediments probably due to fact that the rate of Fe supply is greater than rate of reductive dissolution on the seafloor. The high Fe/Al ratio above upper continental crust is due to additional supply of Fe by aeolian dust, may be from the Indian sub-continent. This is evident in GC-01R, which is much closer to the Indian subcontinent has comparatively high Fe and Fe/Al ratio than in the GC-03. The highest Fe/Al ratio at ~12 ka (Glacial Termination-1) in these two sediment cores is similar to the southeastern Arabian Sea sediment cores (Rao et al., 2010; Pattan et al., 2012).

Formatted: Font: 12 pt, Complex Script Font: 12 pt

### 3.3.2 Cerium and Ce/Ce\*

Formatted: Font: 12 pt, No underline, Font color: Auto, Complex Script Font: 12 pt

Cerium is an unusual member of lanthanide group due to its dual oxidation states ( $Ce^{3+}$  and  $Ce^{4+}$ ). Under oxidizing condition,  $Ce^{3+}$  is oxidized to  $Ce^{4+}$ , which is less soluble, and under suboxic/anoxic conditions,  $Ce^{4+}$  is reduced to  $Ce^{3+}$  (Elderfield, 1988; de Baar et al., 1988). This allows Ce to deviate from the regular behavior shown by other strictly trivalent lanthanides, and can be used to track the redox conditions of depositional environments (German and Elderfield, 1990; Pattan et al., 2005). The Ce/Ce\* values can be  $<1$ ,  $>1$  and  $\approx 1$  which indicate negative, positive and no anomaly respectively (Murray et al., 1991). The negative Ce/Ce\* anomaly ( $< 1$ ) is due to the presence of calcareous, siliceous organisms, phillipsites, phosphorites, smectite and/or reducing conditions (Piper, 1974a & b; Courtois and Jaffrezic-Renault, 1977; Desprairies and Courtois 1980; Tlig and Steinberg 1982; Banakar et al., 1998; Pattan et al., 2005). The positive Ce/Ce\* anomaly is due to presence of the  $Ce^{4+}$  enriched Fe-Mn oxyhydroxides, reflecting oxic conditions (Piper, 1974b). Finally, the absence of a Ce/Ce\* anomaly (neither positive nor negative) is due to dominance of terrigenous material (Nath et al., 1992).

Formatted: Font: 12 pt, Complex Script Font: 12 pt

Formatted: Font: 12 pt, No underline, Font color: Auto, Complex Script Font: 12 pt

The bulk Ce concentration in GC-01R varies from 31 to 73 ppm with an average of 53 ppm and in GC-03, ranges from 52 to 74 ppm with an average of 63 ppm. The slight increase in Ce content in GC-03 could be due to its location at the base of OMZ. The lowest bulk Ce content occurs during last deglaciation and Heinrich events may indicate reducing conditions (Fig. 4). Comparatively high Ce content between 14 to 10 ka probably reflect less reducing or improved oxygenation condition. This is also corroborated by the increased concentration of Mn and Fe in both the cores. The Ce/Ce\* anomaly in both sediment cores is negative, varying from 0.76 to 0.92 (Fig. 4). Over the last ~10 ka, Ce/Ce\* varies from 0.80 to 0.85 and between ~14 and 10 ka, it increased to ~ 0.90. During last deglaciation and Heinrich events, Ce/Ce\* anomaly is more negative (Fig.4) indicating intense reducing conditions, and is corroborated with Mn/Al and Fe/Al. Interestingly, between ~10 and 14 ka, Ce/Ce\* values are closer to 1, with a flat shale-

Formatted: Font: 12 pt, Complex Script Font: 12 pt

Formatted: Font: 12 pt, No underline, Font color: Auto, Complex Script Font: 12 pt

normalized lanthanide pattern. This is due to increased influence of terrigenous material. The high terrigenous material is associated with high sedimentation rate and occurred during important events like the cool Younger Dryas and warm Bølling-Allerød period (Fig. 4).

Formatted: Font: 12 pt, Complex Script Font: 12 pt

The Ti/Al ratio in the marine sediments has been used to trace aeolian dust supply in the Eastern Mediterranean (Wehausen and Brumsack, 2000), Arabian Sea (Schnetger et al., 2000). Globally, average aeolian deposition rates were 3-5 times higher during glacial periods than in interglacials (Rea, 1994). Ti/Al ratio in GC-01R varies from 0.060 to 0.090 with an average of 0.075 and in GC-03 ranges from 0.060 to 0.086 with an average of 0.072 (Fig. 6). The highest Ti/Al ratio of 0.090 and 0.086 in both the sediment cores recorded during ~ 14 and 10 ka, suggest increased input of aeolian dust. The slightly higher Ti/Al ratios recorded in GC-01R compared to GC-03 could be due to dust blown from the Indian sub-continent into the EAS. Ti/Al ratio recorded in these two sediment cores (0.060 to 0.090) is higher than the Ti/Al ratio of aeolian dust from Arabian Peninsula (0.057 to 0.062) reported in northeastern Arabian Sea (Sindh continental margin) sediments from 571m water depth (Deplazes et al., 2014).

Formatted: Font: 12 pt, No underline, Font color: Auto, Complex Script Font: 12 pt

### 3.3.3 Molybdenum

Formatted: Font: 12 pt, Complex Script Font: 12 pt

Molybdenum (Mo) concentration in the Earth's crust is very low (~1 ppm; McLennan, 2001) but is the most abundant transition metal in the modern oxygenated ocean (105 nM), present as molybdate ( $\text{MoO}_4^{2-}$ ), and conservative in oxic environments (Collier, 1985) with a residence time of ~800 ka (Emerson and Husted, 1991). The removal of Mo from the ocean to the underlying sediments is driven largely by redox conditions and to some extent by microbially removed. Under oxidizing conditions, Mo is generally associated with Mn oxyhydroxide phases with a nearly constant Mo/Mn ratio of 0.002 (Shimmield and Price, 1986; Crusius et al., 1996; Tribovillard et al., 2006) and this phase constitutes ~ 35-50 % of total Mo removal (Scott et al., 2008; Poulson Brucker et al., 2009). In the presence of hydrogen sulfide, even at very low concentrations (~10  $\mu\text{M}$   $\text{H}_2\text{S}$ ), molybdate converts into particle reactive thiomolybdate ( $\text{MoS}_4\text{-xO}^{2-}$ ) and is rapidly adsorbed on to organic matter and authigenic sulfide minerals (Helz et al., 1996; Crusius et al., 1996; Ericson and Helz, 2002; Algeo and Lyons 2006; Helz et al., 2011; Scott and Lyons, 2012). Piper (1994) and Crusius et al. (1996) suggested that high Mo concentrations (e.g., 5 to 40 ppm) in sediments indicate highly reducing overlying water column (i.e., anoxic conditions). Recently, Scott and Lyons (2012) suggested that in the euxinic environment, where hydrogen sulfide is present in the water column, and depending upon the availability of Mo in the water column, the sediments show Mo enrichment of >60 to 100 ppm whereas, if sulfide is restricted to sediment pore waters then Mo concentration in

Formatted: Font: 12 pt, No underline, Font color: Auto, Complex Script Font: 12 pt

Formatted: Font: 12 pt, Complex Script Font: 12 pt

Formatted: Font: 12 pt, No underline, Font color: Auto, Complex Script Font: 12 pt

the sediment will be ~ 10 ppm. Molybdenum concentrations in sediments and sedimentary rocks can therefore provide information about redox conditions at the time of sediment deposition (Calvert and Pedersen, 1993; Crusius et al., 1996, 1999; Dean et al., 1997; 1999; Zheng et al., 2000; Yarincik et al., 2000; Werne et al., 2002; McKay and Pedersen, 2014).

Formatted: Font: 12 pt, Complex Script Font: 12 pt

Molybdenum concentration in GC-01R vary from 0.7 to 27 ppm with an average of 3.1 ppm and in GC-03, ranges from 0.46 to 3.5 ppm with an average of 1.35 ppm suggesting its enrichment compared to lithogenic background value of ~ 1 ppm (Fig.4). In GC-01R, the average Mo content over the last 14 ka is 1.4 ppm and increased to 6-13 ppm (8 ppm average) during the last deglaciation with a spike of 27 ppm at 14.4 ka (Fig.4). Over all, Mo content is low in GC-03 compared to GC-01R. The mean Mo content in the EAS is enriched compared to surface sediments extending from above to well below the OMZ off Pakistan margin (avg. 0.9 ppm) and at a sub-surface depth of 30-35 cm (avg. 1.1 ppm) (Crusius et al., 1996) and from the Southeastern Arabian Sea (< 1 ppm) (Pattan and Pearce, 2009). The Mo concentration in sediments from modern sulfidic settings covering wide range varies from 1 ppm to 100s of ppm. The Mo concentration is distinctly different in the sediments where hydrogen sulfide is confined to sediment pore-waters and sulfidic bottom waters (Scott and Lyons, 2012). In the presence of sulfide and thiomolybdates in the sediment pore-waters, the sediment average Mo content is ~ 10 ppm and rarely exceeds 20 ppm. On the contrary, in euxinic environment where hydrogen sulfide is present in the water column, then the Mo content ranges from 60-100 ppm (Scott and Lyons, 2012). In the EAS average Mo content is less than 10 ppm suggesting non-euxinic environments with a presence of hydrogen sulfide in the sediment pore-waters. However, during the last 14 ka (Holocene, Younger Dryas and Bølling-Allerød) the Mo concentration in the sediment is just above the crustal abundance indicating trace of hydrogen sulfide in the pore waters whereas high Mo content (6-13 ppm) during last deglaciation and Heinrich events suggest presence of more hydrogen sulfide in the pore-waters.

Formatted: Font: 12 pt, No underline, Font color: Auto, Complex Script Font: 12 pt

The primary sink for  $\text{MoO}_4^{2-}$  in the oxic environment is co-precipitation/adsorption with Mn-oxyhydroxides where Mo/Mn ratio should be ~0.002 (Shimmield and Price, 1986). In both the sediment cores, the Mo/Mn ratio is quite high (0.02 to 0.25) and distribution of Mo and Mn are quite different in the sediment cores suggesting Mo is not associated with Mn-oxyhydroxide phases. Mo concentrations in GC-03 is just close to crustal abundance during the last 16 ka and then increased from 1 to 3.5 ppm during 32 to 16 ka suggesting presence of hydrogen sulfide in the sediment pore-waters. Therefore, GC-01R core is under more reducing conditions compared to GC-03. The Mo/Al ratio is also higher as expected in GC-01R (0.07 to 1.86) compared to GC-03 (0.005 to 0.35) and mimic the bulk Mo distribution (Fig 4).

Formatted: Font: 12 pt, Complex Script Font: 12 pt

Formatted: Font: 12 pt, No underline, Font color: Auto, Complex Script Font: 12 pt

Formatted: Font: 12 pt, Complex Script Font: 12 pt

The positive correlation between  $C_{org}$  and Mo observed in many black shales, and modern sediments deposited in oxygen-deficient marine basins is well known and suggests that scavenging with organic matter is a principal mechanism by which sediments become enriched in Mo (Brumsack 1986; Wilde et al., 2001; Werne et al., 2002; Lyons et al., 2003; Cruse and Lyons 2004; Algeo and Lyons 2006, Algeo et al., 2007; Scott et al., 2008; Gill et al., 2011; Helz et al., 2011). According to Helz et al., (1996), availability of dissolved sulfide is also a critical factor for Mo sequestration and simultaneous accumulation of organic carbon may generate hydrogen sulfide on a local and basinal scale. The sulfide can occur either in pore waters or in the water column (Lyons et al., 2003). The highest  $C_{org}$  content was recorded during late Holocene in both the cores (Fig. 3) but Mo concentration is low during this time (Fig. 4). In contrast, during the last deglaciation, and Heinrich events though  $C_{org}$  content is low (~1 wt%) but Mo concentration reaches maximum (Fig.3 & 4). The scatter plot of Mo versus  $C_{org}$ , does not show any correlation in both the cores ( $r^2=0.09$ ) (Fig. 7; Table 3 & 4). This is contrary to the general observation made by other researchers. The absence of covariance between  $C_{org}$  and Mo could suggest that  $C_{org}$  may not be the only control on Mo uptake into sediments (Gilleaudeau and Kah, 2013). The apparent absence of covariance between Mo and  $C_{org}$  was also observed in some Proterozoic euxinic shales (Scott et al., 2006, 2008) and drill core sediments of Atar group from Africa (Gilleaudeau and Kah, 2013). This could also be due to low Mo concentrations in the water column. On the other hand, the absence of any correlation between  $C_{org}$  and Mo may suggest that Mo enrichment is related to decreased ventilation rather than increased productivity (Ivanochko and Pedersen, 2004; Cartapanis et al., 2011). Therefore, the absence of covariance between  $C_{org}$  and Mo content in EAS might be due to a combination of factors such as nature of  $C_{org}$ , and changes in ventilation control sedimentary redox conditions.

Formatted: Font: 12 pt, No underline, Font color: Auto, Complex Script Font: 12 pt

Formatted: Font: 12 pt, Complex Script Font: 12 pt

Formatted: Space After: 6 pt, Line spacing: 1.5 lines

### 3.3.5 Uranium

Uranium (U) is conservative in oxygenated oceanic waters and has a residence time of ~0.5 Ma (Ku et al., 1977; Cochran, 1982; Chen et al., 1986; Dunk et al., 2002). Dissolved U in seawater has a concentration of ~13 nM (Chen et al., 1986) and is present as an uranyl tricarbonate species ( $UO_2(CO_3)_3^{4-}$ ) in the oxic seawater. Under reducing condition,  $U^{6+}$  is converted to  $U^{4+}$ , which is

Formatted: Font: 12 pt, No underline, Font color: Auto, Complex Script Font: 12 pt

Formatted: Justified, Space After: 6 pt, Line spacing: 1.5 lines

Formatted: Font: 12 pt, Complex Script Font: 12 pt

Formatted: Font: 12 pt, No underline, Font color: Auto, Complex Script Font: 12 pt

Formatted: Space After: 6 pt

particle reactive, and adsorbed on the sediment or clay mineral surface (Klinkhammer and Palmer, 1991; Tribovillard et al., 2005). The association of U with the particulate organic carbon suggests that U may serve as a proxy for organic carbon transport to the seafloor (Kumar et al., 1995; Anderson et al., 1998; Zheng et al., 2002). Under suboxic and anoxic conditions, U shows strong enrichment above the upper continental crust and also exhibits a positive correlation with Mo (Zheng et al., 2000). Therefore, U concentration in marine sediments is used extensively to trace the paleo-redox conditions of the depositional environment (Dean et al., 1999; Algeo and Maynard, 2004; Tribovillard et al., 2008; Algeo et al., 2012).

Formatted: Font: 12 pt, Complex Script Font: 12 pt

Uranium concentration in GC-01R varies from 5 ppm to 23 ppm with an average of 10 ppm whereas, in GC-03, it ranges from 6 to 17 ppm with an average of 11 ppm. Thus, the U content in both the sediment cores is very similar and enriched ~ 4 times compared to upper continental crust (3 ppm: Taylor and McLennan, 1995). GC-01R, has U content of ~ 12 ppm during Holocene and reduced to ~ 6 ppm during 14-10 ka but increased to maximum of 23 ppm during last deglaciation. This could be due to intense reducing conditions during last deglaciation. Similarly, high U content during last deglaciation and Heinrich events is also recorded in GC-03. High U content is observed in the surface sediments from the east-west transect within the OMZ at a water depth ranging from 218m to 325m in the EAS (Nath et al., 1997). On the contrary, low U content is recorded in a deep sea sediment core from the southeastern Arabian Sea during the last 100 ka (Pattan and Pearce, 2009). Sarkar et al., (1993) reported enrichment of organic carbon and  $^{238}\text{U}$  of 8 dpm/gm during the last glacial period (~18 ka) and proposed near anoxic conditions caused by the deep water circulation in the southeastern Arabian Sea. However, such near anoxic conditions are not possible in the Arabian Sea because there is no extreme enrichment of either U nor Mo concentration. Uranium enrichment and its association with relatively high organic carbon was due to changes in circulation pattern in the southeastern deep Arabian Sea (Pattan and Pearce, 2009).

Formatted: Font: 12 pt, No underline, Font color: Auto, Complex Script Font: 12 pt

Jones and Manning (1994) suggested that U/Th ratio of  $< 0.75$  is indicative of an oxic depositional environment. In GC-01R, U/Th ratio varies from 0.8 to 3 and 0.8 to 1.6 in GC-03, indicating sediments were never exposed to oxic conditions. High U/Th ratio is recorded during last deglaciation and Heinrich events reflecting an intense reducing conditions. Normally, authigenic U and organic carbon show a positive correlation suggesting U removal by organic carbon (Kumar et al., 1995; Anderson et al., 1998; Zheng et al., 2002). On the contrary, no such correlation is observed in both cores (Fig. 8, Table 3 & 4) indicating  $C_{\text{org}}$  may not be the only carrier of U in the sediments. Scatter plot of U against calcium carbonate shows good positive correlation for GC-01R ( $r^2=0.78$ ) and reasonably good in GC-03 ( $r^2=0.28$ ) (Fig.9; Tables 3 & 4). This may be due to

Formatted: Font: 12 pt, Complex Script Font: 12 pt

Formatted: Font: 12 pt, No underline, Font color: Auto, Complex Script Font: 12 pt

incorporation of U into carbonate skeletons. The incorporation of U probably taking place during the journey of foraminifera in the water column. Relatively high U concentrations were observed in carbonates from deeper part of the Gulf of Mexico (Mo et al., 1971). It is observed that high U content in calcareous skeletons was due to presence of aragonite compared to calcite (Kitano and Oomori, 1971). Therefore, in EAS aragonite may be the major contributor for the bulk calcium carbonate content (Naidu et al., 2013; Naik and Naidu, 2016).

### **3.4 Process responsible for the development of intense reducing condition**

Sarkar et al., (1993) proposed near anoxic conditions in the deeper part of the southeastern Arabian Sea at a water depth 2500m during the entire last glacial cycle (MIS- 2, 3 and 4) associated with high organic carbon and authigenic U content and was probably caused by the change in deep water circulation. More recently, Pattan and Pearce (2009) suggested suboxic conditions during the LGM, stadials of MIS-5b, 5d, and Glacial Termination-II in southeastern Arabian Sea. Piotrowski et al. (2009) studied the Nd isotopic composition of leached authigenic ferromanganese oxides and  $\delta^{13}\text{C}$  of benthic foraminifera in a deep-sea sediment core from the equatorial Indian Ocean at a water depth of 3800m, showed a decreased contribution from North Atlantic Deep Water (NADW) during MIS-2 & 4. Therefore, it appears that in the deep southeastern Arabian Sea and equatorial Indian Ocean, suboxic conditions during the last glacial period were due to a change in the circulation and is associated with increased  $C_{\text{org}}$  (Sarkar et al., 1993; Pattan and Pearce, 2009; Piotrowski et al., 2009). Based on redox-sensitive element concentration and their ratios such as low Fe/Al, Mn/Al, high U/Th, Mo/Al and strong negative Ce/Ce\* anomaly during last deglaciation and Heinrich events indicate an intense reducing conditions in the EAS. However, the cause behind the development of intense reducing conditions appear to be different when compared to the deep southeastern Arabian Sea. The intense reducing conditions during the last deglaciation in the EAS is associated with high U and Mo concentrations, but with low  $C_{\text{org}}$  (~1 to 2 %) content. The positive correlation between  $C_{\text{org}}$ , Mo and U content that is typically observed in reducing sediments (Algeo and Lyons, 2006) is not observed in sediments of EAS (Fig. 6 & 7). The absence of any such correlation between  $C_{\text{org}}$ , U and Mo suggest that productivity may not be responsible for the development of reducing conditions in the OMZ of EAS. It has also been suggested that increased sedimentation rate and a corresponding decreased oxygen flux into the sediment can result in anoxic conditions (McKay and Pedersen, 2014). However, there is no increase in the sedimentation rate during deglaciation and Heinrich events (Fig. 2), so this is ruled out as a cause for the Mo and U enrichments in these cores. The strongest contender is the ventilation related to the movement of oxygen deficient Subantarctic Mode Waters - Antarctic Intermediate Waters (SAMW-AAIW) in the

Formatted: Font: 12 pt, Complex Script Font: 12 pt

Formatted: Font: 12 pt, No underline, Font color: Auto, Complex Script Font: 12 pt

Formatted: Font: 12 pt, Complex Script Font: 12 pt

Formatted: Font: 12 pt, No underline, Font color: Auto, Complex Script Font: 12 pt

EAS. Similar to the present study, during the deglaciation, enrichment of Mo, Re and Cd was reported in the eastern tropical North Pacific Ocean sediment cores and was due to oxygen depleted SAMW-AAIW (Hendy and Pedersen, 2006). Recently, Brain et al. (2010) reported the presence of  $^{14}\text{C}$ -depleted intermediate waters during deglaciation at a water depth of 596m and 820m from the northern Arabian Sea ( $18^\circ\text{N}$ ) off the Oman Coast. A similar observation was made in the eastern north Pacific Ocean near Baja California (Marchitto et al., 2007; Stott et al., 2009) and they suggested that the intermediate waters are oxygen depleted SAMW-AAIW. The evidence for this comes from Nd isotopic studies of fish teeth (Basak et al., 2010) where a deglacial decrease in  $\epsilon_{\text{Nd}}$  values is interpreted to represent an influx of AAIW into the north eastern Pacific Ocean, which coincides with negative radiocarbon excursions (Marchitto et al., 2007; Scott et al., 2009). The negative radiocarbon excursions at the northern Arabian Sea observed by Bryan et al., (2010) at  $18^\circ\text{N}$  is due to oxygen depleted intermediate waters and same water mass might have extended upto  $15^\circ\text{N}$ , where both sediment cores from EAS are situated. Therefore, the intense reducing conditions developed during deglaciation and Heinrich events in the EAS could be due to the presence of oxygen depleted SAMW-AAIW.

Formatted: Font: 12 pt, Complex Script Font: 12 pt

The intense reducing conditions recorded during last deglaciation and Heinrich events in both of the sediment cores have important implications with respect to lanthanide fractionation. Lanthanide fractionation can be studied using ratio of shale-normalized Lanthanum to Yttrium ( $\text{La}_{(n)}/\text{Yb}_{(n)}$ ). The Ce/Ce\* anomaly in both cores is  $<1$  suggesting reducing conditions (Fig. 4). The intense reducing condition observed during the last deglaciation is associated with a strong negative Ce/Ce\* anomaly in both the sediment cores. There is a large variations in the  $\text{La}_{(n)}/\text{Yb}_{(n)}$  ratio ranging from 0.8 to 1.35 in the cores (Fig. 10). In both the sediment cores the  $\text{La}_{(n)}/\text{Yb}_{(n)}$  ratio is  $<1$  during the last 10 ka suggesting depletion of the light lanthanide compared to the heavy lanthanide, whereas between 14 and 10 ka this ratio is almost constant and is close to 1, indicating the presence of terrigenous derived material (Piper, 1973; Nath et al., 1992). During last deglaciation and Heinrich events, the  $\text{La}_{(n)}/\text{Yb}_{(n)}$  ratio is  $>1$  and reaches a maximum of 1.35 whereas Ce/Ce\* becomes more negative, reaching lowest value of  $\sim 0.75$ . This suggests that heavy lanthanides are removed during intense reducing conditions. Therefore, intense reducing conditions during last deglaciation and Heinrich events in the EAs might have been caused by the presence of oxygen depleted water mass from SAMW-AAIW and might be responsible for the lanthanide fractionation.

Formatted: Font: 12 pt, No underline, Font color: Auto, Complex Script Font: 12 pt

Formatted: Font: 12 pt, Complex Script Font: 12 pt

Formatted: Justified, Space After: 6 pt, Line spacing: 1.5 lines



#### 4. Conclusions

The following conclusions are drawn from the present study:

- There exist three types of depositional environment in the sediments of EAS. Holocene sediments (last 10 ka) were deposited under weakly reducing conditions, 14 to 10 ka (Younger Dryas and Bølling-Allerød) were also under reducing conditions but dominated by the increased terrigenous material. And last deglaciation and Heinrich events were under intense reducing conditions. The highest  $C_{org}$  and Ba/Al ratio occurred during late Holocene (last 6 ka) suggesting higher productivity but is not associated with high Mo and U content. On the contrary, sediments deposited during the last deglaciation and Heinrich events have lowest  $C_{org}$  and Ba/Al ratio (low productivity) but associated with highest Mo and U enrichment. There is no traditional positive correlation of  $C_{org}$  with U and Mo in both sediment cores, reflecting productivity may not have an impact on the development of reducing conditions within the OMZ of EAS. The intensification of reducing conditions during the last deglaciation and Heinrich events could be due to ventilation of bottom waters resulting from the inflow of oxygen depleted SAMW-AAIW.
- Mo enrichment in both the sediment cores suggest non-euxinic environments in EAS with the presence of hydrogen sulfide within the sediment pore-waters. GC-01R has more reducing conditions due to its location within the core of OMZ compared to GC-03. Behaviour of Mo in GC-03 does not match with other redox-sensitive elements distribution. This could be due to  $H_2S$  content remained below or very close to the threshold for the enrichment of Mo.
- There is a distinct lanthanide fractionation where  $L_{a(n)}/Y_{b(n)}$  ratio is  $<1$ ,  $\sim 1$  and  $>1$  during Holocene, terrigenous dominated sediment and last deglaciation and Heinrich events in the EAS sediments respectively.

#### 5. Acknowledgements

Formatted: Font: 12 pt, No underline, Font color: Auto, Complex Script Font: 12 pt

Formatted: Justified, Space After: 6 pt, Line spacing: 1.5 lines

Formatted: Font: 12 pt, Complex Script Font: 12 pt

Formatted: Font: 12 pt, No underline, Font color: Auto, Complex Script Font: 12 pt

Formatted: Justified, Space After: 6 pt

Formatted: Font: 12 pt, Complex Script Font: 12 pt

Formatted: Font: 12 pt, No underline, Font color: Auto, Complex Script Font: 12 pt

Formatted: Indent: First line: 0", Space After: 6 pt

Formatted: Font: 12 pt, Complex Script Font: 12 pt

Formatted: Font: 12 pt, No underline, Font color: Auto, Complex Script Font: 12 pt

Formatted: Font: 12 pt, Complex Script Font: 12 pt

Formatted: Font: 12 pt, No underline, Font color: Auto, Complex Script Font: 12 pt

Formatted: Font: 12 pt, Complex Script Font: 12 pt

Formatted: Space After: 6 pt

Formatted: Indent: First line: 0"

Formatted: Space After: 6 pt

Formatted: Font: 12 pt, Complex Script Font: 12 pt

Formatted: Font: 12 pt, No underline, Font color: Auto, Complex Script Font: 12 pt

Formatted: Font: 12 pt, Complex Script Font: 12 pt

Authors are grateful to Director, NIO, Goa for the permission to publish this work. Thanks are due to Dr. V.K.Banakar, for providing AMS dates for the sediment cores, Scientific and Crew members of Akademik Siderenko cruise number 32 for their help and support during the sediment core collection onboard. Authors are grateful to Dr. Konstantin Choumiline and an anonymous reviewer for their constructive comments, and suggestions which helped to improve the quality of manuscript. Thanks are also due to Prof. Ihsan Al-Aasm, Associate Editor, Journal of Marine and Petroleum Geology for his encouragement, Prof. J.G. Pearce, United Kingdom, for editorial corrections, Dr. H. Dalton for the discussions, Dr. C. Prakash Babu for allowing us to use Coulometer, Mr. Milindraj and Mrs. Puja Naik for their assistance during sample processing. This is NIO contribution No.....

Formatted: Font: 12 pt, No underline, Font color: Auto, Complex Script Font: 12 pt

Formatted: Font: 12 pt, Complex Script Font: 12 pt

## References

Formatted: Font: 12 pt, Complex Script Font: 12 pt

- Agnihotri, R., Sarin, M.M., Somayajulu, B.L.K., Bull, A.T.J., Burr, G.S., 2003. Late-Quaternary biogenic productivity and organic carbon deposition in the eastern Arabian Sea. *Paleogeography, paleoclimatology, Paleoecology*. 197, 43-60.
- Algeo, T.J., Lyons, T.W., 2006. Mo-total organic carbon covariation in modern anoxic marine environments: implications for analysis of paleoredox and paleohydrographic conditions. *Palaeoceanography* 21, doi:10.1029. 2004PA001112.
- Algeo, T.J., Maynard, J.B., 2004. Trace-element behavior and redox facies in core shales of upper Pennsylvanian Kanas-type cyclothems. *Chemical Geology*. 206, 289-318.
- Algeo, T.J., Ingall, E., 2007. Sedimentary Corg:P ratios, paleocean ventilation, and Phanerozoic atmospheric pO<sub>2</sub>. *Palaeogeography, Palaeoclimatology, Palaeoecology*. 256, 130-155. doi:10.1016/j.palaeo.2007.02.029
- Algeo, T.J., Rowe, H., 2012. Paleocyanographic applications of trace-metal concentration data. *Chemical Geology* 324-325. doi:10.1016/j.chemgeo.2011.09.002.
- Algeo, T.J., Tribovillard, N., 2009. Environmental analysis of paleocyanographic systems based on molybdenum-uranium covariation: *Chemical Geology*, 268/3-4, p. 211-225.
- Algeo, T.J., Morford, J., Cruse, A., 2012. New applications of trace metals as proxies in marine environments. *Chemical Geology*. 324-325, 1-5.
- Anderson, R.F., Kumar, N., Mortlock, R.A., Froelich, P.N., Dittrich-Hannen, B., Suter, M., 1998. Late-Quaternary changes in productivity of the Southern Ocean. *J. Marine Systems*. 17, 497-514.
- Banakar, V.K., Parthiban, G., Pattan, J.N., Jauhari, P., 1998. Chemistry of surface sediments along a north-south transect across the equator in the central Indian Basin: an assessment of biogenic and detrital influences on elemental burial on the seafloor. *Chemical Geology*. 147, 217-232.
- Banakar, V.K., Oba, T., Chodankar, A.R., Kuramoto, T., Yamamoto, M., Minagaawa, M. 2005. Monsoon related changes in sea surface productivity and water column denitrification in the eastern Arabian Sea during the last glacial cycle. *Marine Geology*. 219, 99-108.

- Basik, C., Martin, E.E., Horikawa, K., Marchitto, T.M., 2010. Southern Ocean source of  $^{14}\text{C}$ -depleted carbon in the north Pacific Ocean during the last deglaciation. *Nature Geoscience*. 3, 770-773.
- Boning, P., Bard, E., 2009. Millennial/centennial-scale thermocline ventilation changes in the Indian Ocean as reflected by argonite preservation and geochemical variations in Arabian Sea sediments. *Geochim. Cosmochim. Acta*. 73, 6771-6788.
- Brumsack, H.J., 1986. The inorganic geochemistry of cretaceous black shales (DSDP Leg 41) in comparison to modern upwelling sediments from the Gulf of California. In: Summerhayes, C.P., Shackleton, N.J. (Eds), *North Atlantic Palaeoceanography*. Geol. Soc. London Spec. Publ., 21, 447-462.
- Bryan, S.P., Marchitto, T.M. and Lehman, S.J., 2010. The release of  $^{14}\text{C}$  depleted carbon from the deep sea during the last deglaciation: Evidence from the Arabian Sea. *Earth Planetary Science Letters*. 298 (1-2), 244-254.
- Calvert, S.E., Pedersen, T.F., 1993. Geochemistry of recent oxic and anoxic marine sediments: implications for the geological record. *Mar. Geol.* 113, 67-88.
- Calvert, S.E., Pedersen, T.F., 2007. Elemental proxies for palaeoclimatic and palaeoceanographic variability in marine sediments: interpretation and application. In: Hillaire-Marcel, C., Vernal, A.D. (Eds.), *Proxies in Late Cenozoic Paleoclimatology*. Elsevier, Amsterdam.
- Canfield, D.E. Thamdrup, B., 2009. Towards a consistent classification scheme for geochemical environments, or why we wish the term 'suboxic' would go away. *Geobiology*. 7 (4), 385-392. Doi.10.1111/1472-4669.2009002014x
- Cartapanis, O., Tachikawa, K and Bard E., 2011. Northeastern Pacific oxygen minimum zone variability over the past 70 kyrs: Impact of biological production and oceanic ventilation. *Paleoceanography*. 26, PA4208, doi:10.1029.2011PA002126
- Chen J. H., Edwards L., Wasserburg G. J., 1986.  $^{238}\text{U}$ ,  $^{234}\text{U}$  and  $^{232}\text{Th}$  in seawater. *Earth Planetary Science Letters*. 80, 241-251.
- Cochran J. K., 1992. The oceanic chemistry of the U and Th series nuclides. In : *Uranium-Series Disequilibrium: Applications to Earth, Marine and Environmental Sciences* (ed. M. Ivanovich and R. S. Harmon), pp. 334-395, Clarendon Press.
- Collier, R.W., 1985. Molybdenum in the Northeast Pacific Ocean. *Limnology and Oceanography*. 30, 1331-1354.
- Courtois, C., Jaffrezic-Renault, N., 1977. Utilization des propriétés échangeuses d ions du dioxyde de lanthane pour l'analyse des lanthanides par activation neutronique. *C.R.Acad. Sci. Paris. Ser.D.284*, 1139-1142.
- Cruse, A. M., Lyons, T., 2004. Trace metal records of regional paleoenvironmental variability in Pennsylvanian (Upper Carboniferous) black shales. *Chemical Geology*. 206, 319-345.
- Crusius, J., Calvert, S., Pedersen, T., Sage, D., 1996. Rhenium and molybdenum enrichments in sediments as indicators of oxic, suboxic and sulfidic conditions of deposition. *Earth Planetary Science Letters* 145, 65-78.
- Crusius, J., Pedersen, T., Calvert, S. E., Cowie, G.L., Oba, T., 1999. A 35 kyr geochemical record from the Sea of Japan of organic matter flux variations and changes in intermediate water oxygen concentrations. *Paleoceanography*. 14, 248-259.
- Danzeglocke, U., Joris, O. and Weninger, B. 2011. CalPal 2007-HuLu. Accessed on 2011-11-09.
- Dean, W.E., Gardner, J.V., Piper, D.Z., 1997. Inorganic geochemical indicators of glacial interglacial changes in productivity and anoxia on the California continental margin. *Geochim. Cosmochim. Acta*. 61, 4507-4518.
- Dean, W.E., Piper, D.Z., Peterson, L.C., 1999. Molybdenum accumulation in Cariaco basin sediment over the last 24 ky: a record of water column anoxia and climate. *Geology*. 27, 507-510.
- de Baar, H.J.W., German, C.R., Elderfield, H., van Gaans, P., 1988. Rare earth element distribution in anoxic waters of the Carioca Trench. *Geochim. Cosmochim. Acta*. 52, 1203-1219.

- Deplazes, G., Luckge, A., Stunt, J-B, W., Patzold, J., Kuhlmann, H., Husson, D., Fant, M., Hang, G.H., 2014. Weakening and strengthening of the Indian monsoon during Heinrich events and Dansgaard-Oscillations. *Paleoceanography*. 29 (20), 99-114.
- Desprairies, A., Courtois, C., 1980. Relation entre la composition des smectite de alteration sous-marine et leur cortege de terres rares. *Earth and Planetary Science Letters* 48, 124-130.
- Dunk R. M., Mills R. A., Jenkins, W. J., 2002. A reevaluation of the oceanic uranium budget for the Holocene. *Chemical Geology*. 190, 45-67.
- Dymond, J., Suess, E., Lyle, M., 1992. Barium in deep sea sediment: a geochemical proxy for productivity. *Paleoceanography*. 7, 163-181.
- Elderfield, H., 1988. The oceanic chemistry of rare earth elements. *Phil. Transaction Royal Society of London*. A325, 105-126.
- Emerson, S.R., Husted, S.S., 1991. Ocean anoxia and the concentrations of molybdenum and vanadium in sea water. *Marine Chemistry*. 34, 177-196.
- Erickson, B.F., Helz, G.R., 2000. Molybdenum (VI) speciation in sulfidic waters: small stability and liability of thiomobeates. *Geochimica Cosmochim. Acta*. 64(7), 1149-1158.
- Froelich, P.N., Klinkhammer, M.L., Bender, M.L., Luedtke, N.A., Heath, G.R., Cullen, D., Dauphin, P., Hammond, D., Hartmann, B., Maynard, V., 1979. Early oxidation of organic matter in pelagic sediments of the eastern equatorial Atlantic: suboxic diagenesis. *Geochim. Cosmochim. Acta*. 43, 1075-1090.
- German, C.R., Elderfield, H., 1990. Application of the Ce anomaly as a paleoredox indicator: the ground rules. *Paleoceanography* 5, 823-833.
- Gill, B.C., Lyons, T.W., Young, S.A., Kump, L.R., Knoll, A.H., Saltzman, M.R., 2011. Geochemical evidence for widespread euxinia in the later Cambrian ocean. *Nature*. 469, 80-83. doi:10.1038/nature09700
- Gilleaudeau G. J., Kah, L.C., 2013. Oceanic molybdenum draw down by epeiric sea expansion in the Mesoproterozoic. *Chemical Geology*. 56, 21-37.
- Gingele, F.X., Zabel, M., Kasten, S., Bonn, W.J., Nurnberg, C.C., 1999. Biogenic barium as a proxy for paeoproductivity: Methods and limitations of application. In: G. Fisher and G. Wefer (Eds), *Uses of proxies in Paleoceanography: Examples from the South Atlantic*. Springer, Berlin, 345-364.
- Helz, G.R., Miller, C.V., Charnock, J.M., Mosselmans, J.F.W., Patrick, R.A.D, Garner, C.D., Vaughan, D.J., 1996. Mechanisms of molybdenum removal from the sea and its concentration in black shales. EXAFS evidence. *Geochim. Cosmochim. Acta*. 60, 3631-3642.
- Helz, G.R., Bura-Nakic, E., Mikac, N., Ciglenceki, I., 2011. New model for molybdenum behavior in euxinic waters. *Chemical Geology* 284, 323-332.
- Hendy, I.L., Pedersen, T.F., 2006. Oxygen minimum zone expansion in the eastern tropical North Pacific during deglaciation. *Geophysical Research Letters*. 33, L20602, doi:10.1029/2006GL025975.
- Ivanochiko, T.S. and Pedersen, T.F., 2004. Determining the influences of Late Quaternary ventilation and productivity variations on Santa Barbara Basin sedimentary oxygenation: a multi-proxy approach. *Quaternary Science Review*. 23, 467-480.
- Jaccard, S.L., Galbraith, E.D., 2012. Large climate-driven changes of oceanic oxygen concentrations during the last deglaciation. *Nature Geoscience*. 5,, 151- 156. Doi.org/10.1029/2003GB002103
- Jones, B., Manning, D.A.C., 1994. Composition of geochemical indices used for the interpretation of paleoredox conditions in ancient mudstones. *Chemical Geology*. 101, 111-129.
- Kitano, Y. and Oomori, T., 1971. The co-precipitation of Uranium with calcium carbonate. *J. Oceanographic Society of Japan*. 27 (1), 34-42.

- Klinghammer, G.P., Palmer, M.R., 1991. Uranium in the oceans: where it goes and why? *Geochim. Cosmochim. Acta.* 55, 1799-1806.
- Ku, T-L., Knauss, K.G., Mathien, G.G., 1977. Uranium in open ocean: concentration and isotopic composition. *Deep Sea Research.* 24, 1005-1017.
- Kuhnt, W., Holbourn, A.E., Hall, R., Zuleva, M., Kase, R., 2004. Cenozoic history of the Indonesian Throughflow. In: *Continent-Ocean Interactions in the East Asian Marginal Seas.* Vol.149. (eds. P.D.Cliff and others). Pp.287-304, AGU Monograph Series.
- Kumar N., Anderson R. F., Mortlock R. A., Froelich P. N., Kubib P., Dittrich-Hannen B., Suter M., 1995. Increased biological productivity and export production in the glacial Southern Ocean. *Nature.* 378, 675-680.
- Le'vy, M., Shankar,D., Andre, J-M., Shenoi, S.S.C., Durand, F., de Boyer Montegut, C., 2007. Basin-wide seasonal evolution of the Indian Ocean's phytoplankton blooms. *J. Geophysical Researc.* 112, C12014. <http://dx.doi.org/10.1029/2007JC004090>.
- Lynn, D.C., Bonatti, E., 1965. Mobility of manganese in diagenesis of deep sea sediments. *Marine Geology.* 3, 457-474.
- Lyons T.W., Werne, J.P., Hollander, D.J., Murray, R.W., 2003. Contrasting sulfur geochemistry and Fe/Al ratios across the last oxic-to-anoxic transition in the Cariaco Basin, Venezuela. *Chemical Geology.* 195, 131-157.
- Madhupratap, M., Prasanna Kumar, M.S., Bhattathiri, P.M.A., Dileep Kumar, M., Raghukumar, S., Nair, K.K.C., Ramaiah, N., 1996. Mechanism of the biological response to winter cooling in the northeastern Arabian Sea. *Nature.* 384, 549-552.
- Marchitto, T.M., Lynch-Stieglita, J., Hemming, S.R., 2005. Deep Pacific CaCO<sub>3</sub> compensation and glacial-interglacial atmospheric CO<sub>2</sub>. *Earth and Planetary Science Letter.* 231, 317-336.
- McKay, J.L., Pedersen,T.F., 2014. Geochemical response to pulsed sedimentation: Implications for the use of Mo as a paleo-proxy. *Chemical Geology.* 382, 83-94.
- McLennan, S.M., 2001. Relationships between the trace element composition of sedimentary rocks an upper continental crust. *Geochemistry, Geophysics, Geosystems.* 9(ISSN:1525-2027) 2 (Paper number 2000GC000109).
- Mekik, F.A., Anderson, R.F., Loubere, P., Francois, R., Richaud, M., 2012. The mystery of the missing deglacial carbonate preservation maximum. *Quat. Sci. Rev.* 39, 60-72.
- Mir Ahmad, I., Pattan, J.N., Matta, V.M., Banakar, V.K., 2013. Variation of paleo-productivity and terrigenous input in the eastern Arabian Sea during the past 100 ka. *J. Geological Society of India.* 81, 647-654
- McManus, J., Berelson, W.M., Severmann, S., Poulson, R.L., Hammond, D.E., Klinkhammer,G.P., Holm, C., 2006.. Molybdenum and uranium geochemistry in continental margin sediments;Paleoproxy potential. *Geochim. Cosmochim. Acta.* 70, 4643-4662.
- Mo, T., Suttle, A.D., Sackett, W.M., 1971. Uranium concentrations in marine sediments. *Geochim. Cosmochim. Acta.* 37 (1), 35-51.
- Morford, J.L., Martin, U, R., Carney, C.M., 2012. Rhenium geochemical cycling: Insights from continental margins. *Chemical Geology.* 324-325, 73-86.
- Murray, R.W., Buchholtz Brink, M.R., Brink, M.R., Gerlach, D.C., Russ III, G.P., Jones, D.L., 1991. Rare earth, major and trace elements in chert from the Franciscan complex and Monterey group, California: assessing REE sources to fine grained marine sediments. *Geochim. Cosmochim. Acta.* 55, 1875-1895.
- Naidu, P.D., Singh , A.D., Ganeshram, R., Bharti, S.K., 2013. Abrupt climate-induced changes in carbonate burial in the Arabian Sea: Causes and consequences. *Geochemistry, Geophysics, Geosystems.* 15, 1398-1406.
- Naik, S.S., Naidu, P.D., 2016. Carbonate preservation during the 'mystery interval' In the northern Indian Ocean. *Geochemical Journal.* 50, 357-362.

- Naik, S.S., Godad, S.P., Naidu, P.D., Tiwari, M., Paropkari, A.L., 2014. Early-to late Holocene contrast in productivity, OMZ intensity and calcite dissolution in the eastern Arabian Sea. *The Holocene*. 24(6), 749-755.
- Naik, D.K., Saraswat, R., Lea, D.W., Kurtarkar, S.R., Mackensen, A. (In press). Last glacial-interglacial productivity and associated changes in the eastern Arabian sea. *Paleogeography, Paleoclimatology, Paleoecology*.
- Nair, R.R., Ittekkot, V., Manganini, S.J., Ramaswamy, R., Haake, B., Degens, E. T., 1989. Increased particle flux to the deep ocean related to monsoons. *Nature*. 338, 749-751.
- Narayana, A.C., Naidu, P.D., Shinu, N., Nagabhusanam, P., Sukhija, B.S. 2009. Carbonate and organic carbon content changes over last 20 ka in southeastern Arabian Sea: paleoceanographic implications. *Quaternary International*. 206, 72-77.
- Nath, B.N., Roelandts, I., Sudhakar, M., Pluger, W., 1992. Trace and rare earth element patterns of the Central Indian Basin sediment related to their lithology. *Geophysical Research Letters*. 19, 1197-2000.
- Nath, B.N., Bau, M., Rao, B.R., Rao, Ch.M., 1997. Trace and rare earth elemental variation in Arabian Sea sediments through a transect across the oxygen minimum zone. *Geochim. Cosmochim. Acta*. 61, 2375-2388.
- Pattan, J.N., Masuzawa, T., Naidu, P.D., Parthiban, G and Yamamoto, Y., 2003. Productivity fluctuations in the southeastern Arabian Sea during the last 140 ka. *Palaeogeography, Palaeoclimatology, Palaeoecology* 193, 575 – 590.
- Pattan, J.N., and Pearce, N.J.G., 2009. Bottom water oxygenation history in southeastern Arabian Sea during the past 140 ka: Results from redox-sensitive elements. *Palaeogeography, Palaeoclimatology, Palaeoecology*. 280, 396-405.
- Pattan, J.N., Pearce, N.J.G., Mislankar, P.G., 2005. Constraints in using Cerium-anomaly of bulk sediments as an indicator of paleo bottom water redox environment: A case study from the Central Indian Ocean Basin. *Chemical Geology*. 221, 260-278.
- Pattan, J.N., Parthiban, G., Gupta, S.M., Ishfaq ,A.M., 2012. Fe speciation and Fe/Al ratio in the sediments of Southeastern Arabian Sea as an indicator of climate change. *Quaternary International*. 250, 19-26.
- Paytan, A., McLaughlin, K., 2007. The oceanic phosphorous cycle. *Chemical Reviews*. 107 (2), 563-576.
- Piper, D.Z., 1973. Origin of metalliferous Sediments from the East Pacific Rise. *Earth Planetary Science Letters*, 19, 75-82.
- Piper, D.Z., 1974a. Rare earth elements in the sedimentary cycle, a summary. *Chemical Geology*. 14, 285-304.
- Piper, D.Z., 1974b. Rare earth elements in ferromanganese nodules and other marine phases. *Geochim. Cosmochim. Acta*. 38, 1007-1022.
- Piotrowski, A.L., Banakar, V.K., Scrivner, A.E., Elderfield, H., Galy, A., Dennis, A., 2009. Indian Ocean circulation and productivity during the last glacial cycle. *Earth and Planetary Science Letters*. 285 (1-2), 179-189.
- Poulson Brucker, McManus, J., Severmann, S., Berelson, W.M., 2009. Molybdenum behavior during early diagenesis: insights from Mo isotopes. *Geochemistry, Geophysics, Geosystems*. 10, <http://dx.doi.org/10.1029/2008GC002180>.
- Prell, W.L., Kutzbach, J.E., 1987. Monsoon variability over the past 150 000 years. *J. Geophysical research*. 92, 8411-8425.
- Rao, V.P., Kessarkar, P.M., Thamban, M., Patil, S.K., 2010. Paleoclimatic and diagenetic history of the late Quaternary sediments in a core from the southeastern Arabian Sea: geochemical and magnetic signals. *Journal of Oceanography*. 66, 133-146.

- Rea, D.K., 1994. The paleoclimatic records provided by eolian deposition in deep sea; The geological history of wind. *Reviews of Geophysics*. 32 (20), 159-195.
- Rosenthal, Y., Boyle, E.A., Labeyrie, L., Oppo, D., 1995. Glacial enrichments of authigenic Cd and U in Subantarctic sediments: a climatic control on the elements oceanic budget?. *Paleoceanography*. 10(3), 395-413.
- Saraswat, R., Lea, D.W., Nigam, R., Mackensen, A., Naik, D.K., 2013. Deglaciation in the tropical Indian Ocean driven by interplay between the regional monsoon and global teleconnections. *Earth Planetary Science Letters*. 375, 166-175.
- Sarkar, A., Bhattacharya, S.K., Sarin, M.M., 1993. Geochemical evidence for anoxic deep water in the Arabian Sea during the last glaciations. *Geochim. Cosmochim. Acta*. 57, 1009-1016.
- Schnetger, B., Brumsack, H.-J., Schale, H., Hinrichs, J., Dittert, L., 2000. Geochemical characteristics of deep-sea sediments from the Arabian Sea: a high-resolution study. *Deep-Sea Research II*. 47, 2735-2768.
- Scholz, F., Severmann, S., McManus, J., Hensen, C., 2014. Beyond the Black Shale paradigm: The sedimentary fingerprint of an open-marine iron shuttle. *Geochim. Cosmochim. Acta*. 127, 368-380.
- Scott, C., Lyons T W., 2012. Contrasting molybdenum cycling and isotopic properties in euxinic versus non-euxinic sediments and sedimentary rocks: Refining the paleoproxies. *Chemical Geology*. 324-325, 19-27.
- Scott, C., Lyons, T.W., Bekker, A., Poulton, S.W., Shen, Y., Chu, X., Anabar, A.D., 2008. Tracing the stepwise oxygenation of the Proterozoic ocean. *Nature*. 452, 456-460.
- Shackleton, N.J., 2000. The 100,000 year ice-age cycle identified and found to lag temperature, carbon dioxide and orbital eccentricity. *Science*. 289, 1897-1902.
- Shimmiel, G.B., Price, N.B., 1986. The behavior of molybdenum and manganese during early sediment diagenesis-offshore Baja California. *Marine Chemistry*. 19, 261-280.
- Singh, A.D., 2007. Episodic preservation of pteropods in the eastern Arabian Sea: Monsoonal changes, Oxygen Minimum Zone intensity and aragonite compensation depth. *Indian J. of Marine Sciences*. 36, 4378-4383.
- Southon, J., Kashgarian, M., Fontugue, M., Metivier, B. and Yim, W.W.S., 2002. Marine reservoir correction for the Indian Ocean and southeast Asia. *Radiocarbon*. 44:,167-180.
- Taylor, S.R., McLennan, S.M., 1985. *The Continental Crust: Its Composition and Evolution*. Blackwell, Oxford. 312 pp.
- Tlig, S., Steiberg, M., 1982. Distribution of rare earth elements (REE) in size fractions of recent sediments of the India Ocean. *Chemical Geology*. 37, 317-333.
- Tribovillard, N., Ramdani, A., Trentesaux, A., 2005. Controls on organic accumulation in upper Jurassic shales of northwestern Europe as inferred from trace metal geochemistry. In: Harris (Ed). *The deposition of organic-carbon-rich sediments: models, mechanism and consequences*. Society for Sedimentary Geology Special Publication, vol. 82, pp.145-164.
- Tribovillard, N., Algeo, T.J., Lyons, T.W., Riboulleau, A., 2006. Trace metal as paleo redox and paleo productivity proxies: an update. *Chemical Geology*. 30, 12-32.
- Tribovillard, N., Lyons, T.W., Riboulleaus, A., Bout-Roumazeilles, V., 2008. A possible capture of molybdenum during early diagenesis of dioxic sediments. *Bulletin de la socieete Geologique de France* 179 (1), 3-12.
- Volat, J.L., Pastouret, L., Vergnaud-Grazzini, I., 1980. Dissolution and carbonate fluctuations in Pleistocene deep-sea cores: a review. *Marine Geology*. 34, 1-28.
- Werne, J.P., Sageman, B.B., Lyons, T.W., Hollander, D.J., 2002. An integrated assessment of a "type euxinic" deposit: evidence for multiple controls on black shale deposition in the Middle Devonian Oatka Formation. *American J. Science*. 302, 110-143.
- Wilde, P., Quinby-Hunt, M.S., Lyons, T. W., 2001. Molybdneum as an indicator of original organic content in ancient anoxic sediments. *Abstr. Programs-Geological. Society America* 33 (6),

- A39. Warning, B., Brumsack, H-J., 2000. Trace metal signatures of eastern Mediterranean sapropels. *Paleogeography, Paleoclimatology, Paleoecology*. 158, 293-309.
- Wyrski, K., 1973. In: Zeitzschel, B. (Ed), *Physical Oceanography of the Indian Ocean: The Biology of the Indian Ocean*. Springer-Verlag, pp. 18-36.
- Yarinick, K.M., Murray, R.W., Peterson, L.C., 2000. Climatically sensitive eolian and hemipelagic deposition in the Cariaco Basin, Venezuela, over the past 578,000 years: results from Al/Ti and K/Al. *Paleoceanography*. 1, 210-228.
- Yuan, W., Liu, G., Stebbins, A., Xu, L., Niu, X., Luo, W., Li, C., 2017 (In Press). Reconstruction of redox conditions during deposition of organic-rich shales of the Upper triassic Yangchang formation, Ordos Basin, China. *Paleogeography, Paleoclimatology Paleoecology*.
- Zheng, Y., Anderson, R.F., Van Gen, A., Kuwabara, J., 2000. Authigenic molybdenum formation in marine sediments: a link to pre water sulfide in the Santa Barbara basin. *Geochim. Cosmochim. Acta*. 64(24), 4165-4178.
- Zheng, Y., Anderson, R.F., van Geen, A., Fleisher, M.Q., 2002. Preservation of particulate non-lithogenic uranium in marine sediments. *Geochim. Cosmochim. Acta*. 66(17), 3085-3092.

**Tables.**

Formatted: Indent: Left: 0"

Formatted: Font: Bold

Formatted: Left

Formatted: Font color: Black



**Table 1.** Details of sediment cores collected from eastern Arabian Sea.

Sed.Core No.	Short name	Latitude (N)	Longitude (E)	Water depth (m)	Core length (m)
ABP-32/GC-01R	GC-01R	15° 29.494`	72° 43.639`	642	4.22
ABP-32/GC-03	GC-03	15° 29.158`	72° 36.925`	1086	3.22

**Table 2.** <sup>14</sup>C dates of two sediment cores (ABP-32/GC-01R, ABP-32/GC-03) from eastern Arabian Sea.

Sediment core No	Core depth (cm)	<sup>14</sup> C age	Cal. Age (BP)
ABP-32/GC-01R	58-60	4665±41	4528 ±68
	124-126	9665±52	10216±25
	200-202	10481±55	11280±48
	256-258	11283±59	12659±67
	340-342	13055±65	14683±331
ABP-32/GC-03	384-386	14262±72	16723±264
	0-2	2268±35	1541±53
	96-98	10620±57	11488±131
	116-118	11285±57	12662±65
	184-186	15051±76	17571±253
	236-238	18940±120	22992±290
	296-298	25720±220	30022±285

Formatted: Font color: Black

**Table 3.** Correlation matrix for the elements analysed including Ce/Ce\* for the sediment core ABP-32/GC-01R. n=101

Formatted: Font: Bold, No underline, Font color: Black

Formatted: No underline, Font color: Black

	<i>C<sub>org</sub></i>	<i>CaCO<sub>3</sub></i>	<i>Al</i>	<i>Fe</i>	<i>Mn</i>	<i>U</i>	<i>Mo</i>	<i>Ce/Ce*</i>	<i>Ba</i>
<i>C<sub>org</sub></i>	1.00								
<i>CaCO<sub>3</sub></i>	-0.14	1.00							
<i>Al</i>	-0.12	-0.83	1.00						
<i>Fe</i>	-0.27	-0.85	0.96	1.00					
<i>Mn</i>	-0.47	-0.74	0.89	0.95	1.00				
<i>U</i>	0.08	0.89	-0.85	-0.88	-0.80	1.00			
<i>Mo</i>	-0.21	0.67	-0.74	-0.67	-0.56	0.59	1.00		
<i>Ce/Ce*</i>	-0.39	-0.82	0.88	0.95	0.94	-0.87	-0.50	1.00	
<i>Ba</i>	0.89	0.09	-0.29	-0.42	-0.58	0.29	0.02	-0.53	1.00

**Table 4.** Correlation matrix for the elements analysed including Ce/Ce\* for the sediment core ABP-32/GC-03. n=80

Formatted: Font: Bold

	<i>C<sub>org</sub></i>	<i>CaCO<sub>3</sub></i>	<i>Al</i>	<i>Fe</i>	<i>Mn</i>	<i>U</i>	<i>Mo</i>	<i>Ce/Ce*</i>	<i>Ba</i>
<i>C<sub>org</sub></i>	1.00								
<i>CaCO<sub>3</sub></i>	0.43	1.00							
<i>Al</i>	-0.60	-0.69	1.00						
<i>Fe</i>	-0.59	-0.82	0.79	1.00					
<i>Mn</i>	-0.73	-0.75	0.66	0.85	1.00				
<i>U</i>	-0.13	0.53	-0.23	-0.34	-0.39	1.00			
<i>Mo</i>	0.29	0.06	-0.38	-0.03	0.01	-0.16	1.00		
<i>Ce/Ce*</i>	-0.69	-0.89	0.72	0.81	0.91	-0.47	-0.08	1.00	

Ba 0.32 -0.09 0.26 -0.02 -0.37 0.10 -0.49 -0.23 1.00

Fig. 1

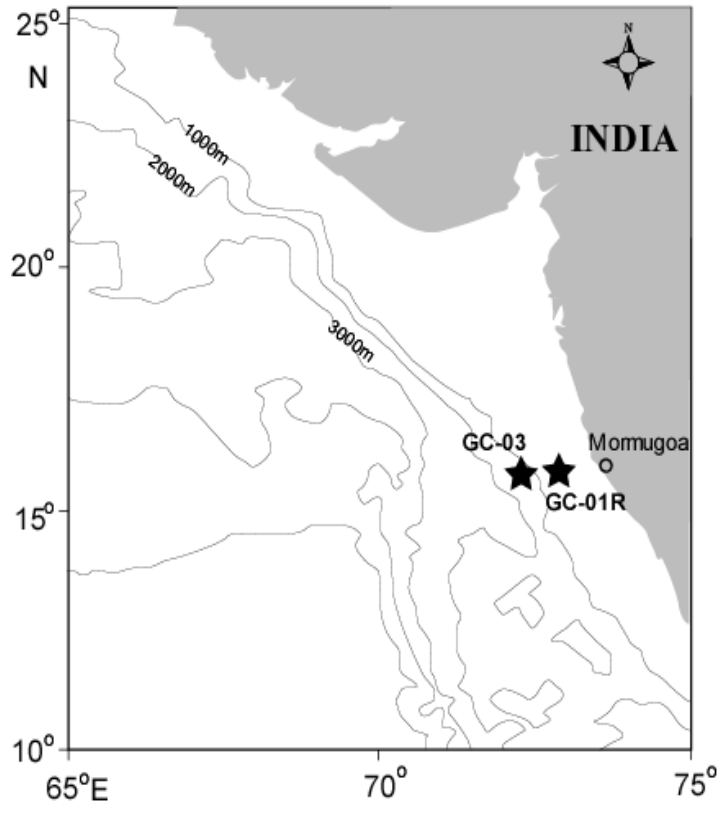


Fig. 2

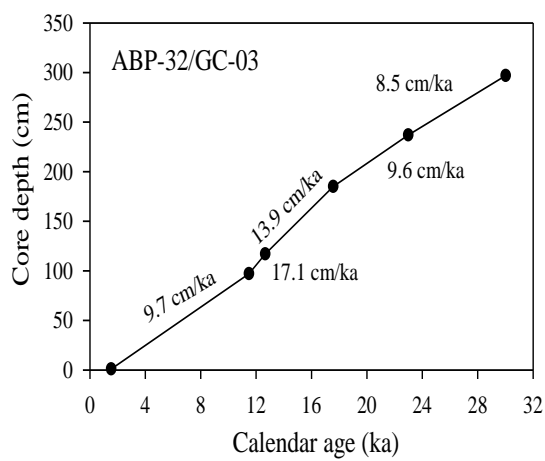
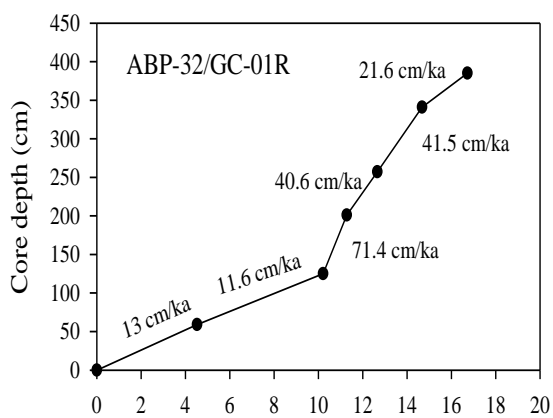


Fig.3

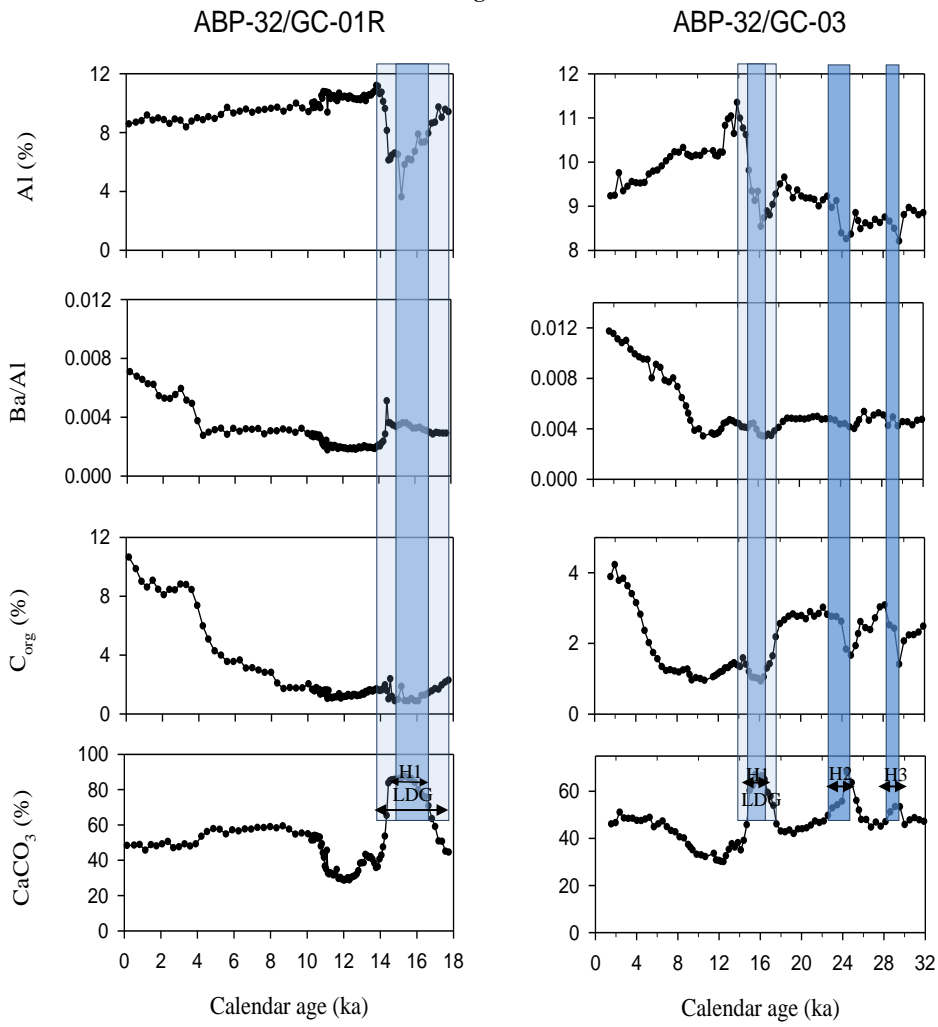
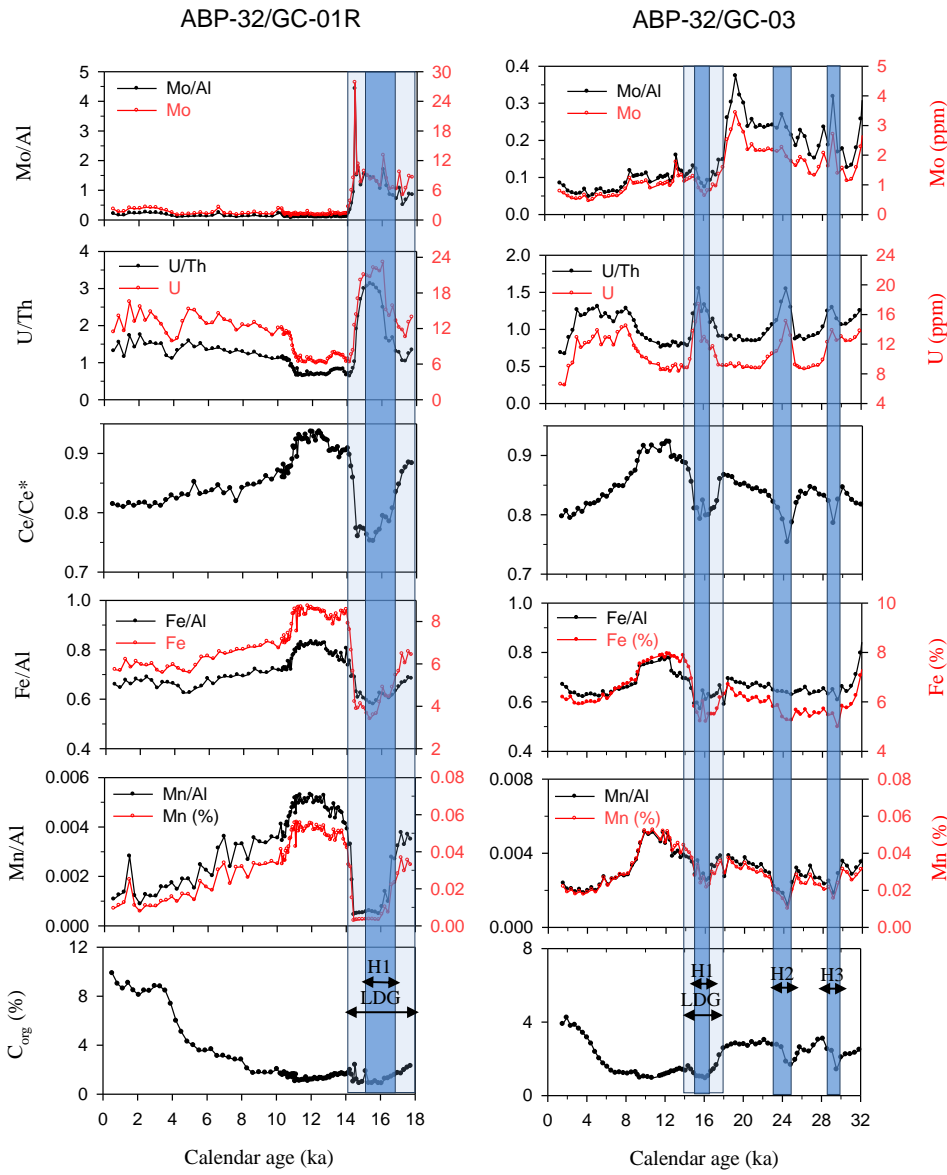
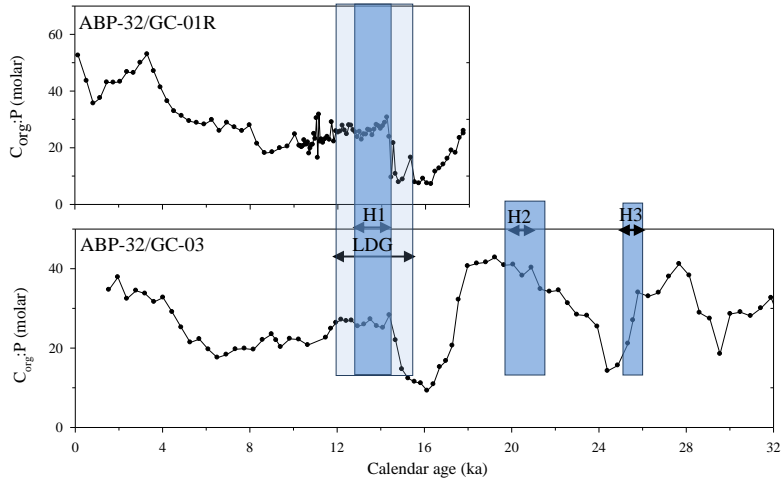


Fig. 4



**Fig. 5**



Formatted: Left

Formatted: Left

**Fig. 6**

Formatted: Left

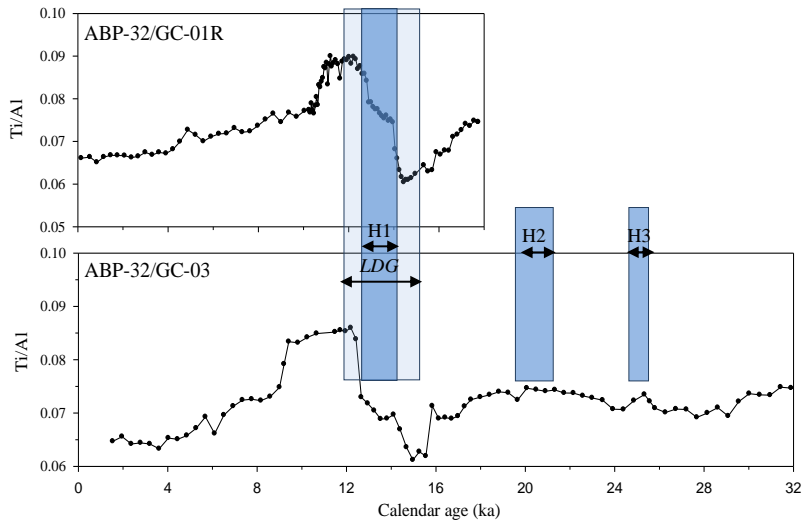


Fig. 7



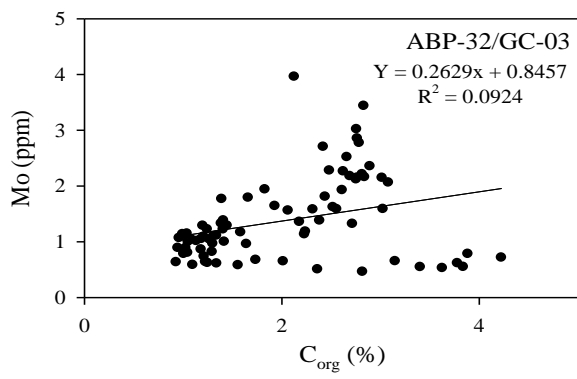
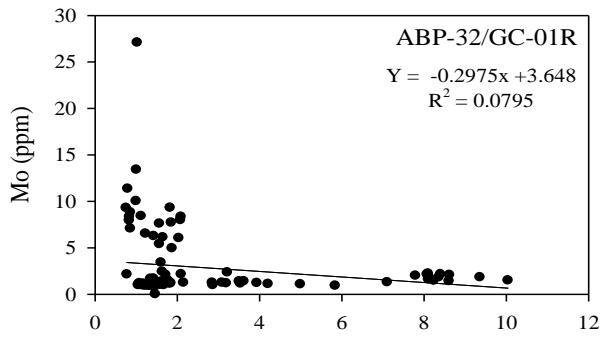
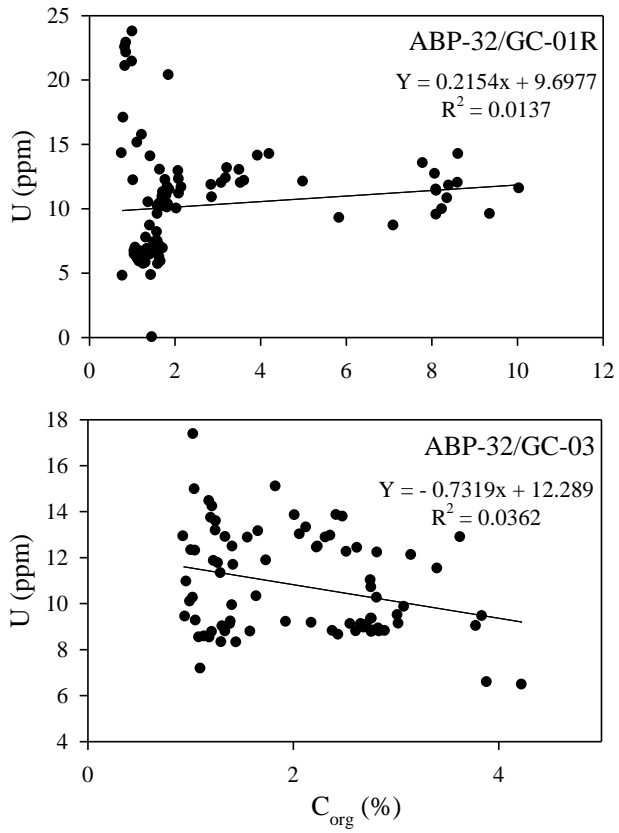


Fig.8



**Fig. 9**

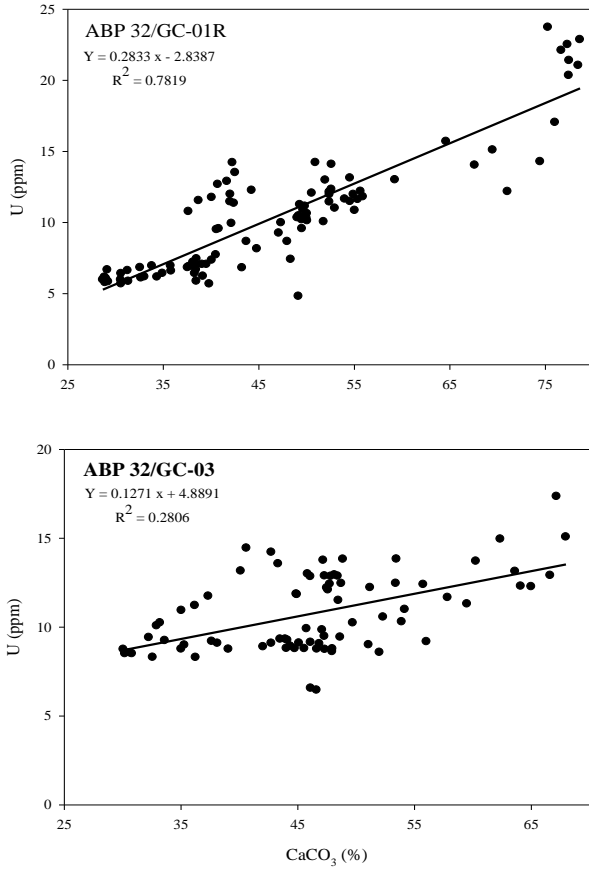
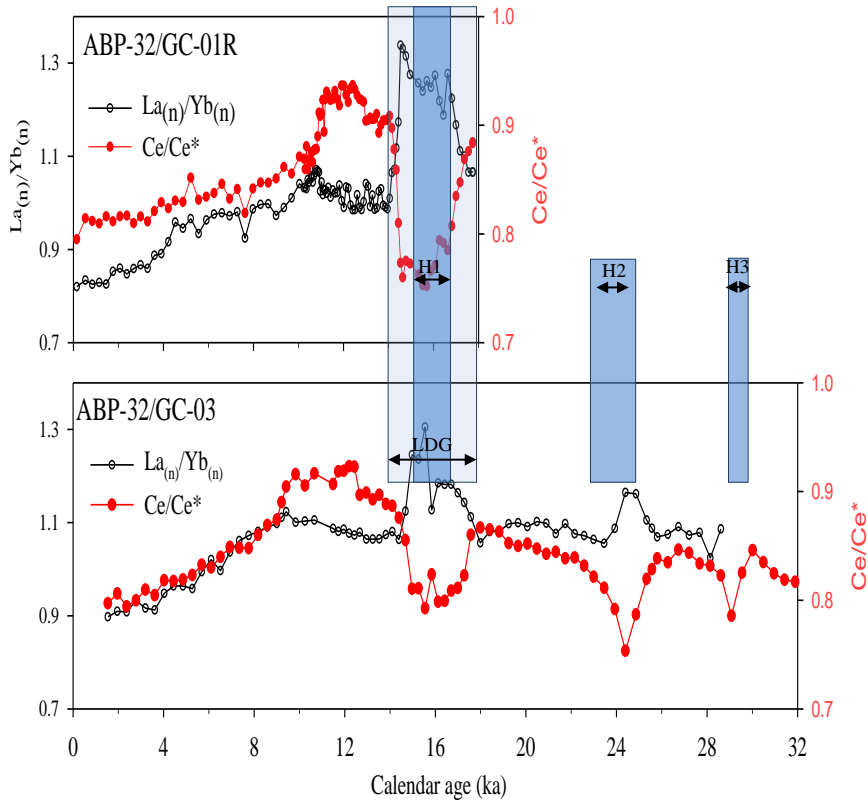


Fig. 10



Formatted: Left

### Caption for the figures

**Fig. 1.** Map showing location of two sediment cores (ABP-32/GC-01R, ABP-32/GC-03) in the EAS.

First sediment core (642m) is within the centre of OMZ and second core (1086m) is at the base of present day OMZ.

Formatted: Font: Bold

**Fig. 2.** Scatter Plot of depth (cm) against calendar age (ka) for the sediment core ABP-32/GC-01R (top) and ABP-32/GC-03 (bottom) from EAS.

Formatted: Font: Bold

**Fig. 3.** Distribution of productivity proxies such as calcium carbonate,  $C_{org}$ , Ba/Al and Al (terrigenous representing element) for sediment core ABP-32/GC-01R (left side) and ABP-32/GC-03 (right side). LDG- last deglaciation, H1, H2, H3 are Heinrich Events.

Formatted: Font: Bold

**Fig. 4.** Distribution of  $C_{org}$  (%), bulk Mn (%), Fe (%), U (ppm) and Mo (ppm) concentration and Mn/Al, Fe/Al, Ce/Ce\*, U/Th and Mo/Al for the sediment core ABP-32/GC-01R (left side) and ABP-32/GC-03 (right side).

Formatted: Font: Bold

**Fig. 5.** Distribution of  $C_{org}$  :P Molar ratio in both the sediment cores. (Note that Redfield ratio is 106).

Formatted: Font: Bold

**Fig. 6.** Distribution of Ti/Al ratio for the sediment core ABP-32/GC-01R (top) and ABP-32/GC-03 (bottom).

Formatted: Font: Bold

**Fig. 7.** Scatter plot of  $C_{org}$  (%) against Mo (ppm) for the sediment core ABP-32/GC-01R (top) and ABP-32/GC-03 (bottom).

Formatted: Font: Bold

**Fig. 8.** Scatter plot of  $C_{org}$  (%) against U (ppm) for the sediment core ABP-32/GC-01R (top) and ABP-32/GC-03 (bottom).

Formatted: Font: Bold

**Fig. 9.** Scatter plot of Calcium carbonate (%) against U (ppm) for the sediment core ABP-32/GC-01R (top) and ABP-32/GC-03 (bottom).

Formatted: Font: Bold

**Fig. 10.** Distribution of Ce/Ce\* and  $La_{(n)}/Yb_{(n)}$  for the sediment cores ABP-32/GC-01R (top) and ABP-32/GC-03 (bottom).

Formatted: Font: Bold